Text S1

Abstract. This document provides further documentation on the 41-year inventory of vegetation fire emissions constructed for the RETRO project ("REanalysis of the TROpospheric chemical composition over the past 40 years"), a global modeling study to investigate the trends and variability of tropospheric ozone and other air pollutants over the past decades. Fires are an important and highly variable source of air pollutant emissions in many world regions and they constitute a significant if not dominant factor controlling the interannual variability of the atmospheric composition. The GBC paper which is refering to this document as supplementary online material describes the background and state-of-the-art for estimating global fire emissions, provides a brief description of the methodology used for constructing the RETRO inventory, and presents and discusses the resulting data set and its uncertainties. Here, we provide detailed information on the models, the data and parameters used in each continental-scale region and we discuss our choices in the context of results from earlier and recent studies, including some critical analysis about the possible causes for the large differences observed. The complete data set of vegetation fire emissions is made available through the web sites of the Global Emissions Inventory Activity (GEIA, http://geiacenter.org/) and the RETRO project (http://retro.enes.org/emissions/).

1. Introduction

Reliable estimation of emissions from wildland fires requires detailed knowledge about the fuel type, fuel composition, the fire behaviour, and the amount of material burned. Even a single fire is a very dynamic process, and it is spatially heterogeneous down to a very fine scale. It is difficult to obtain robust average values for fuel and fire properties, and the more parameters are treated explicitely, the larger the uncertainties become (Robinson, 1989). The problem is aggravated, because many of the individual fire parameters are correlated. For example, a fire with high available fuel load will generally burn with higher intensity and thus more completely. Higher wind speeds will lead to higher fire intensities and a more rapid spread, which generally implies larger burned areas as well. While there is a wealth of information on individual fires or fires on a regional level, there is only little consistency between such studies, and scarce information on continental or even global scales. Nevertheless, researchers have attempted to produce global inventories of fire emissions using statistical information on biomass loads, fuel properties, and fire behaviour, and, more recently, estimating burned areas with the help of satellite data from different coarse resolution instruments (e.g. the Advanced Very High Resolution Radiometer (AVHRR), the Along Track Scanning Radiometer (ATSR), the SPOT-VEGETATION, or Moderate Resolution Imaging Sensor (MODIS)). These sensors have often been designed for different purposes, and the detection of active fires or burned scars is therefore limited (e.g. Boschetti et al., 2004).

In this study, we compile a global-scale inventory of wildland fire emissions covering the four decades from 1960 to 2000. Due to the scarcity of reliable quantitative information for many world regions, this inventory must rely on different assumptions and methodologies. The general methodology consists of three steps: (1) obtain estimates of annual burned areas and the seasonality of fire scars on continental-scale levels, (2) assign a carbon flux estimate to all fires of a specific ecosystem, and (3) compute emission fluxes for trace gases and aerosol compounds through application of emission ratios suitable for the ecosystem. Among the different sources of input data were many scientific articles, officially reported fire statistics and reports from the Global Fire Monitoring Center (http://www.gfmc.org), satellite data sets (mostly GBA2000), other global emission inventories (GWEM and GFED), and a numerical model, which simulates fire occurence and fire spread on a regional scale (Reg-FIRM). This online supplement provides detailed information on the tools and data sets used in the main article of this study and it discusses the choice of parameters for each region of the RETRO global wildland fire inventory. It can well be seen as a rather thorough review of the recent literature and may therefore be of use as a benchmark for future inventory activities.

This document is structured into four sections following this introduction. We begin with a description of the modelling tools Reg-FIRM and GWEM (sections 2 and 3), then we discuss fires in the boreal and midlatitude zones (section 4), and in the tropical and subtropical zones (section 5). A short concluding section ends this document.

2. The regional fire model (Reg-FIRM)

The scarcity of reliable burnt area data for the period 1960-2000 necessitated the use of simulated data on fire activity to complement other, more regional-focused fire data sets and correlation methods used in this study. A reparameterized version of the so-called regional fire model, Reg-FIRM (*Venevsky et al.,* 2002) was used to simulate area burnt globally, 1960-2000, at a monthly time step and spatial resolution of 0.5°. Reg-FIRM simulates general fire dynamics based on semi-physical models of fire spread (after *Telitsyn,* 1996), explicitly considers different ignition sources, and is designed for fire simulation within coarse resolution grid cells; in this case, approximately 2500 km^2 at the equator. The fire model runs within the Lund-Potsdam-Jena Dynamic Global Vegetation Model (LPJ-DGVM) (*Sitch et al.,* 2003), modified subsequently by *Gerten et al.* (2004) to include a new soil-water balance module.

LPJ simulates the phenology, population and carbon dynamics of eight tree Plant Functional Types (PFTs) and

0886-6236/08/$12.00

two grass PFTs at a spatial resolution of 0.5°(refer Table 1). The coupling of the fire model to LPJ allows dynamic feedbacks between fire and vegetation. Reg-FIRM returns information to LPJ on the relative proportion of PFT cover reduced by fire, based on the product of i) PFT-specific fire-induced mortality rates, ii) the simulated number of fires (dependent on climatic fire danger and both human and lightning-caused ignitions) in a grid cell, and iii) the average size of a fire in a grid cell.

Reg-FIRM was developed and originally applied to the Iberian Peninsula for the period 1974 to 1994, and it produced results that were correlated, both spatially and temporally with observed fire statistics (*Venevsky et al.,* 2002). Further testing shows that it captures observed fire activity reasonably well in the Australian Wet-Dry tropics (*Spessa et al.,* 2003; *Zwenzner,* 2004), Brandenburg, Germany (*Thonicke and Cramer,* 2006) and in the western USA (*Vogel,* 2004), so long as appropriate local parameterizations are used.

The parameter values and input data used to run the coupled fire-vegetation model reflected environmental conditions present within different biomes during the simulation period. As input to LPJ, monthly fields of mean temperature, precipitation, rain days and cloud cover were taken from the UK Climate Research Unit (CRU) TS 2.0 (1901-2002) monthly climate database on a 0.5°global grid (*Mitchell et al.,* 2003). CO_2 concentrations were derived from a database of historical global atmospheric CO_2 concentrations (Carbon Cycle Model Linkage Project, *McGuire et al.,* 2001). These data were derived from a combination of ice core measurements (*Etheridge et al.,* 1996) and atmospheric observations (*Keeling et al.,* 1996). The dataset was extended using observations from Mauna Loa Observatory, Hawaii (*Keeling and Whorf,* 2005). Soil texture data are derived from the FAO soil database (*Zobler,* 1986; *FAO,* 1991).

Reg-FIRM uses daily temperature differences and upper soil moisture values derived from the soil-water balance module in LPJ to simulate daily Fire Danger Index (FDI). The product of monthly FDI and the sum of the potential number of human- and lightning-caused ignitions per month is used to simulate the actual number of fires per grid cell per month. The two main input variables governing fire activity in Reg-FIRM, not otherwise needed by LPJ, are i) wind speed, which is used to drive forward rate of fire spread, and thus area burnt simulations; and ii) population density, used as a basis for calculating the potential number of human-caused ignitions per grid cell. Monthly average wind speed data (1960-2000) were derived from NCEP Reanalysis data provided by the NOAA-CIRES Climate Diagnostics Center, Boulder, Colorado, USA, (http://www.cdc.noaa.gov/). Global population density data for the years 1950, 1970, 1990 and 2000 were obtained from the HYDE 3.0 database (*Goldewijk,* 2005; http://www.rivm.nl/hyde/). Annual population densities for each grid cell were calculated by linear interpolation. Information about the key parameters used to run Reg-FIRM are given in Table 1.

We have analysed the burned area results from the Reg-FIRM simulations and found that they generally provide a reasonable description of the seasonality and inter-annual variability of fires in savanna regions. Absolute values of Reg-FIRM burned areas are less reliable and we therefore applied scaling factors to these results in some regions (see detailed discussion below). In addition to the model evaluation for the Iberian peninsula, Northern Germany, Northern Australia and the Western US (*Venevsky et al.,* 2002; *Spessa et al.,* 2003; *Zwenzner,* 2004; *Thonicke and Cramer,* 2006; *Vogel,* 2004) we compared the Reg-FIRM results with multi-annual estimates by *Barbosa et al.* (1999) for Africa (see section 5.1 below and Figure 1 in the main article). Generally, maxima and minima coincide quite well, although they do not always match.

3. The Global Wildfire Emissions Model (GWEM)

The Global Wildfire Emissions model was developed at the time when the first global burned area satellite products became available (*Simon et al.,* 2004; *Tansey et al.,* 2004), and it is based on the idea of making explicit use of satellite data to the extent possible, so that aggregated parameters only need to be used for fuel load estimates and emission factors. The model is described by *Hoelzemann et al.* (2004) and *Hoelzemann* (2006), so we will only give a brief summary here and list in particular the changes that were made to GWEM for this study.

GWEM 1.2 (this is the version of the model published in *Hoelzemann et al.,* 2004) was based on the GLOBSCAR burned area data set from ESA-ESRIN (*Simon et al.,* 2004). This data set retrieves burned areas via two different algorithms applied to the 1 km data of the Along Track Scanning Radiometer (ATSR) on board the ERS-2 satellite. The first algorithm (K1) is a contextual algorithm based on the geometrical characteristics of the burned pixels in the near infrared and thermal infrared, while the second algorithm (E1) applies a series of fixed threshold tests to data of four spectral channels (*Simon et al.,* 2004). In GWEM each burn scar is processed individually according to the vegetation type at its location. The vegetation classes are taken from the MODIS-IGBP data set of *Friedl et al.,* (2002). Fuel loads were estimated based on simulation results with the Lund-Potsdam-Jena (LPJ) dynamic vegetation model (*Sitch et al.,* 2003) using literature values for defining the fractions of the different carbon pools (litter, leaf, wood, and fine roots) that are available for combustion. The LPJ plant functional types were mapped onto the MODIS IGBP vegetation classes in order to obtain separate fuel load estimates for forest or savanna burning within the same LPJ grid cell.

Final steps in the calculation of emissions are the estimate of combustion completeness (or burning efficiency, cf. *Reid et al.,* 2005), and the application of emission factors (*Andreae and Merlet,* 2001, with updates from M.O. Andreae, personal communication, 2005). Total direct carbon emissions for the year 2000 were reported as 1741 TgC, while CO emissions were estimated as 271 Tg CO. As with the inventory from this study, GWEM does not take into account domestic biofuel use, charcoal making, and agricultural waste burning emissions. This must be kept in mind when comparing the results with other literature estimates.

For the present study, we use an updated version (1.4) of GWEM, which is based on burned areas from the SPOT VEGETATION sensor (GBA 2000, *Tansey et al.,* 2004). For the region of South America GBA2000 burned areas were replaced by a data set from CPTEC/INPE (http://www.cptec.inpe.br/queimadas/), because it was found that GBA2000 severely underestimates burning in the tropical forests. The CPTEC/INPE data set is based on a combination of AVHRR and GOES/ABBA satellite derived fire pixels. These are converted to burned area as described in *Prins et al.* (1996, 1998).

GWEM 1.4 also includes a more detailed description of carbon pools from the LPJ model and uses improved fuel load estimates (*Hoelzemann,* 2006). For each of 5 ecosystem types in GWEM, the available fuel load is computed as

$$AFL_k = \sum_{t=1}^{n} pftf_{c_t} \cdot \sum_{p=1}^{npools} m_{t,p} \cdot \chi_{k,t,p} \qquad (1)$$

Table 1. Key parameter values and inputs used by Reg-FIRM to simulate monthly area burnt at 0.5°, globally 1960-2000

Parameter	Value(s)	Comments and References
Fuel threshold (below which no fires are simulated)	0.1 kg/m2 biomass	In most ecosystems, a fuel load less than about 0.1 kg/m^2 is insufficient for sustained fire spread (*Pyne et al.,* 1996)
Moisture of extinction (governs fuel moisture conditions too marginal for sustained burning)	Grasses = 30%; Trees= 25%	*Thonicke et al.* (2001), *Catchpole* (2002)
Proportion of PFT-survival post-fire	Tropical broadleaved evergreen tree (0.6); tropical broadleaved raingreen tree (0.8); temperate needleleaved evergreen tree (0.7); temperate broadleaved evergreen tree (0.8); temperate broadleaved summergreen tree (0.7); boreal needleleaved evergreen tree (0.2); boreal needleleaved summergreen tree (0.12); boreal broadleaved summergreen tree (0.2); C3 grass (0.01); C4 grass (0.01)	Assumed to be constant throughout, as Reg-FIRM does not simulate fire intensity as a basis for calculating fire-induced mortality in trees. Tropical evergreen trees (*Cochrane,* 2003), tropical raingreen trees and C4 grasses (*Cheney et al.,* 1993; *Williams et al.,* 2002); temperate trees, and C3 grasses (*Merida,* 1999); boreal trees (*Goldammer and Furyaev,* 1996)
Fuel bulk density (kg/m^2)	Tropical broadleaved evergreen tree (18); tropical broadleaved raingreen tree (12); temperate needleleaved evergreen tree (25); temperate broadleaved evergreen tree (12); temperate broadleaved summergreen tree (22); boreal needleleaved evergreen tree (18); boreal needleleaved summergreen tree (16); boreal broadleaved summergreen tree (16); C3 grass (2); C4 grass (2)	Tropical evergreen and raingreen trees, C4 grasses (*Cheney et al.,* 1993; *Williams et al.,* 2002); temperate trees, C3 grasses (*Merida,* 1999); Boreal trees (*Goldammer and Furyaev,* 1996)
Fire duration	1 day	Assumed to be constant throughout, as no quantitative data on spatio-temporal variability exists globally, 1960-2000. Value used is a conservative estimate provided by *Venevsky et al.* (2002)
Potential number of lightning-caused ignitions	5% of total number of fires	Assumed to be constant throughout. Data on lightning-caused fires are either simply not available or highly uncertain for most regions across the globe. Hence, the value used is a conservative average following "best estimate" data provided in *Pyne et al.* (1996), *Williams et al.* (2002), and *Goldammer and Furyaev* (1996)
Potential number of ignitions produced by one human per fire season day	Regionally dependent	Long-term observed fire data needed to calculate potential human-caused ignition rates (PHIR) (*Venevsky et al.,* 2002) are limited to very few regions around the globe. Consequently, we took existing PHIR values, calculated as part of previous Reg-FIRM studies in specific regions in the humid tropics, tropical savannas, and mediterranean, boreal and temperate zones (*Venevsky et al.,* 2002; *Thonicke and Cramer,* 2006, *Spessa et al.,* 2003; *Zwenzner,* 2004; *Vogel,* 2004; Spessa unpublished data), and extrapolated them through time and across similar major biome and land use types to produce a global PHIR surface. Where required, total numbers of fires were adjusted downwards by 5% to discount lightning-caused fires before calibration

where AFL_k is the available fuel load in ecosystem k, $npft$ denotes the number of plant functional types in LPJ (e.g. 9), f_{c_t} is the fractional cover of PFT t within a grid cell, $npools$ is the number of carbon pools (now 5, since the wood pool has been split into heartwood and sapwood), $m_{t,p}$ is the mass of carbon stored in carbon pool p of PFT t, and $\chi_{k,t,p}$ describes the fire susceptibility, which is defined according to typical burning patterns in specific ecosystems. Further details on GWEM can be found in *Hoelzemann* (2006).

Because of the limited availability of input data, GWEM only provides emission estimates for the year 2000. In this study we therefore use GWEM almost exclusively for obtaining the geographical patterns and seasonality of fires in various regions, while the quantitative estimates of burned area and net carbon emissions stems from different sources. We stratified the GWEM results into the three vegetation classes of this study (forest, wooded, and grassland) and derived the spatial and temporal patterns for each of these classes independently.

4. RETRO inventory parameters for boreal and midlatitude fires

Boreal forest fires occur in Canada, Alaska, and Siberia between May and September, but in some cases fires have also been reported later in the season. In the boreal ecosystems fires play a vital role for the stand structure and function (*Stocks et al.,* 2003; *French et al.,* 2003). Individual fires are often of high energy, consuming several thousand ha and releasing more than 10 tons of carbon per ha into the atmosphere (*Amiro et al.,* 2001).

The majority of large fires in boreal North America is caused by lightning strikes. According to *Stocks et al.* (2003), 66% of all fires between 200 and 1000 ha are caused by lightning. For fires greater than 1000 ha, this fraction increases to 83%. The large fires often occur in remote areas, where the probability for human ignition is low and fire fighting is difficult to impossible. Much less data are available for fires in boreal Eurasia, but the general assumption of lightning as the dominant source for ignition must be questioned here (see below).

4.1. North America

In Canada and Alaska, the large boreal fires (greater 200 ha) represent more than 97% of the total area burned even though they account for less than 3% of all fires (*Stocks,* 1991). For Canada, a database of large fires (LFDB, available at http://fire.cfs.nrcan.gc.ca/research/-climate_change/lfdb_e.html) from 1959 onward has been compiled, and we make explicit use of these data for our inventory. Variability of burned areas in Canada and Alaska is huge: according to *Stocks et al.* (2003) the minimum total annual burned area in Canada over the past 40 years was 165,353 ha (1963) whereas the maximum value was 2,758,149 ha (1961). The burned area for the year 2000 was obtained from the Global Fire Monitoring Center (GFMC) and is estimated as 632,396 ha.

We assume an average carbon release of 15 tC/ha, which corresponds well with the "average severity" carbon release reported by *Kasischke et al.* (2005) and with the average direct carbon release of 13 tC/ha reported by *Amiro et al.* (2001). For simplicity, all Canadian fires are attributed to the "forest" class. The resulting total carbon emissions average at 24 TgC/year and range from 2.5 TgC/year (year 1963) to 91 TgC/year (year 1995). These estimates generally agree to better than 30% with the estimates of *Amiro et al.* (2001) (Figure 1). The discrepancies are largest for the most severe fire years. This is a consequence of our neglect of variability in fire parameters other than burned area. Large stand replacing fires tend to experience a more complete combustion so that the carbon release per ha is higher under these circumstances. Furthermore, in some regions the consumption of soil organic matter can make an important contribution to the net carbon emissions. However, figure 1 clearly shows that the continental-scale emissions variability is predominantly driven by the variation in burned area and therefore gives some justification to our approach.

For Alaska *French et al.* (2003) report burned areas of less than 30,000 ha (1970, 1982, 1989, and 1995) up to 1,500,000 ha (1957). These statistics are incomplete in particular for years prior to 1970. Data on individual fire locations in Alaska exist (*Kasischke et al.,* 2005; http://agdc.usgs.gov/data/blm/fire/index.html) but they were not available to us at the time when the inventory was prepared. We therefore constructed and distributed individual fires randomly from the total burned area estimates of *French et al.* (2003) as described in section 2.2 of the main text. For the years with missing data (1961-1967) we adopted a conservative estimate of 50,000 ha, and for 2000 we prescribed a burned area of 400,000 ha based on qualitative statements of the year 2000 fire season from the US National Interagency Fire Center (NIFC).

The average fire size was assumed to be 800 ha, which is about the same magnitude as the median of the Canadian large fires as reported in the LFDB. 80% of the fires in Alaska were assigned to the "forest" class, and 20% were labeled as "wooded". The respective total carbon emissions per ha are set to 25 and 15 tC/ha. These values are within the range given by *French et al.* (2003) (9.4 tC/ha - 30.1 tC/ha) and they reflect the large contribution of soil organic matter (*French et al.,* 2003; *Kasischke et al.,* 2005). The total carbon release from fires in Alaska thus calculated ranges from 0.19 TgC/year to 23 TgC/year with an average value of 3.8 TgC/year, which is 15 % lower than the estimate of *French et al.* (2003). Maximum emissions are 40 % lower than their estimate, however.

The seasonality of fires in Canada and Alaska has been taken from the Canadian large fire data base (Figure 2). According to this data set fires are significant from May to August with the largest contribution to the total annual burned area in June. This pattern is consistent with the fire danger rating described by *Stocks et al.* (1998), but it differs markedly from the seasonality predicted by Reg-FIRM or GWEM and the GBA2000 data set, which attribute the maximum burned area to the month of August.

For the US, the NIFC posted a list with historical burned areas and some outstanding fire events. Caution must be exercised in using these data, because they may underestimate fires in sparsely populated areas where aerial monitoring was not performed systematically (W.M. Hao, personal communication, 2001). After 1994, burned area information is available on a state level, but we do not make use of this information in order to simplify the approach and ensure consistency of the long-term data set. In order to estimate historic emissions from US fires, we subtract the Alaska burned areas reported by *French et al.* (2003) from the total burned areas reported by the NIFC after we verified that their respective values are consistent for Alaska between 1994 and 1999.

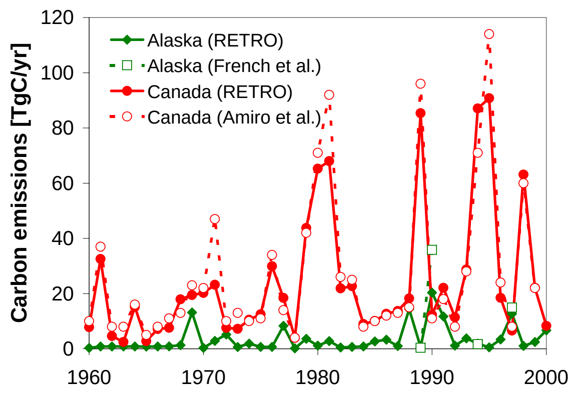

Figure 1. Comparison of total direct carbon emissions from fires in Canada and Alaska with literature values from *Amiro et al.* (2001) and *French et al.* (2003)

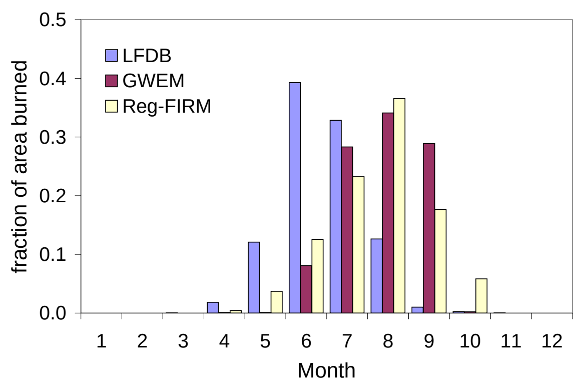

Figure 2. Seasonality of large fires in Canada: Comparison of normalized monthly area burned data from the Canadian large fire data base, GWEM 1.4 (i.e. GBA 2000), and Reg-FIRM

Table 2. Comparison of total carbon emissions from fires in North America estimated by GFED version 2 and from this inventory. Units are TgC/year

Year	GFEDv2	this study
1997	24.4	25.8
1998	111.7	70.0
1999	61.7	39.4
2000	34.8	35.7

Table 3. Comparison of CO emissions from North America. Re-computed values of *Duncan et al.* (2003) versus the estimates from this study. Units are Tg(CO)/year. No data are given for years with limited availability of TOMS aerosol data (see discussion in *Duncan et al.,* 2003)

Year	Duncan et al., 2003	this study
1979	11.0	12.8
1980	11.5	18.4
1981	16.7	18.9
1982	10.1	6.3
1983	9.8	7.8
1984	9.7	3.0
1985	10.0	5.2
1986	9.6	5.2
1987	12.3	5.1
1988	6.5	10.3
1989	14.9	22.2
1990	—	11.0
1991	10.0	9.5
1992	9.6	4.5
1993	—	10.1
1994	—	26.9
1995	—	25.3
1996	—	7.4
1997	6.9	6.2
1998	21.5	18.2
1999	14.5	7.8
2000	—	7.7

We assume that 60% of the total burned area originates from forest fires, and 40% is due to shrubland fires ("wooded" ecosystems). Net carbon emissions are set to 10 and 5 tC/ha, respectively, and the average burned area per fire is assumed to be 600 ha and 400 ha, respectively. The seasonality of US fires is obtained independently for forest and shrubland ecosystems from GWEM 1.4. According to this model, fire emissions in the US peak in September (almost 50% of the annual total). The fires are distributed randomly in the area west of 85°W. This precludes the false attribution of fires along the East coast, which are relatively rare.

According to our inventory, the minimum total carbon emissions from US fires occured in 1991 (1.3 TgC/year), and maximum emissions are estimated for the year 2000 (19.9 TgC/year). Average emissions are 9.4 TgC/year. For comparison, GWEM 1.4 estimates annual total carbon emissions for the US south of 48°N for the year 2000 of 11 TgC, which is about a factor of two lower than our estimate and the average "Temperate North America" emissions listed by *Kasischke et al.* (2005) in their Table 1 of the supporting online material.

Table 2 compares total carbon emissions from the North American continent from our inventory with the results of the Global Fire Emissions Database (GFED) version 2 by *van der Werf et al.* (2006) and Table 3 compares the RETRO CO emissions with re-computed data of *Duncan et al.* (2003). While there is reasonable agreement with the former, the relationship with the latter is somewhat poorer.

4.2. Northern Asia

Emissions from historic fires in Russia are extremely difficult to estimate, because of incomplete aerial surveillance and other reporting problems in particular for years before 1995 when the first satellite data sets became available (*Stocks,* 2004). Even when remote sensing data are used, considerable uncertainties remain (cf. *Goldammer et al.,* 2004). *Boschetti et al.* (2004) compare two different satellite-derived burned area products for the year 2000 and find a factor of two difference in the region of Siberia, Mongolia, and Northern China. Yet, this difference is small compared to the factor of five discrepancy between satellite-derived burned areas and reports from aerial surveillance by

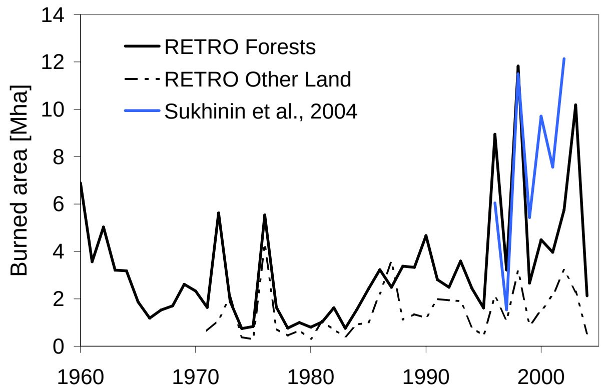

Figure 3. Interannual variability of the burned area in Russian forests and other land types according to a new data set by the Russian ministry of natural resources. The data have been scaled by a factor of 5 to make them consistent with satellite-derived values from *Sukhinin et al.* (2004, shown as grey line)

Table 4. Comparison of burned areas for Siberia from *Soja et al.* (2004) and *Sukhinin et al.* (2004) with the estimates for Russia and Mongolia from this study. Units are 10^6 ha

Year	*Soja et al.*, 2004	*Sukhinin et al.*, 2004	this study
1996	-	6.05	11.1
1997	-	1.54	4.3
1998	10.34	11.49	15.0
1999	6.88	5.43	3.6
2000	9.00	9.71	6.0
2001	8.10	7.56	6.1
2002	11.17	12.14	9.0

Avialesookhrana (*Goldammer,* 2003; *Conard et al.,* 2002). For the severe fire year of 1998, *Conard et al.* (2002) estimate a total burned area of 13.3 Mha in Siberia and contrast this with Avialesookhrana data yielding a total of only 2.9 Mha over an area monitored by aircraft and constituting about 66% of the total forest area in Russia. In a recent publication based on a multi-step processing of AVHRR data, *Sukhinin et al.* (2004) give an average burned area of 7.7 Mha for the time period 1996-2002. For this study, we use a new data set of reported burned areas compiled by the Russian Ministry for Natural Resources and made available to us via the Global Fire Monitoring Center (GFMC). This data set lists annual burned areas for forests from 1960 to 2004 and for other land areas from 1971 to 2004 (Figure 3). The average burned area between 1996 and 2002 from this data set is 1.6 Mha. In order to achieve consistency with the estimates based on remote sensing data, we scale the reported burned area values with a factor of 5. Non-forest burned areas before 1971 are set to a constant value of 1 Mha. Total burned areas then range from 1.2 to 15.6 Mha with an average of 4.7 Mha. This is qualitatively consistent with the assertion of *Kasischke et al.* (2005) that the Asian boreal zone contributes about 3-times as much burned area as the boreal zone on the North American continent.

There is a pronounced difference in the trend of burned area in recent years between the AVHRR based estimates by *Sukhinin et al.* (2004) and the data set from the Russian ministry (see Figure 3 and Table 4). While the former observe a general increase in fire affected forest area (which appears to be consistent with increased fire danger due to drought conditions), this trend is not reflected in our data set. One possible explanation for this might be the decreased level of aerial surveillance in recent years due to lack of funding (*Goldammer,* 2006).

Due to our choice of the region definition, we implicitely assume that Mongolian fires are included in the Russian estimate, and we also include the part west of the Ural mountains. Since we do not further increase our burned area estimates to account for these regions, our estimate are likely biased low.

Due to the pronounced seasonal progression of Russian fires from south to north (*Kasischke et al.,* 2005), we process fires in Northern and Central Asia separately in two latitude bands of 45-60°N and 60-80°N. Lacking more detailed information, we assume that 70% of the total burned area is located south of 60°N. This is qualitatively consistent with the fire maps displayed in *Soja et al.* (2004) and *Sukhinin et al.* (2004). The fires are distributed randomly within the different ecosystem types. For the random distribution of Russian fires (see section 2.2 of the main text) we assume average burned areas of 1000, 800, and 400 ha for forests, shrublands, and grasslands, respectively. Carbon consumption is set to 20, 10, and 3 tC/ha, respectively, which is in the range of values given by *Soja et al.* (2004). *Goldammer et al.* (2004) estimate average net (immediate) carbon release of 4–15 tC/ha for surface fires and 15–20 tC/ha for stand replacing crown fires, while they give a value of 2–3 tC/ha for grassland and shrub fires. If the ecosystem specific burned area exceeds 3 Mha, we increase the carbon consumption for forests and wooded areas to 25 and 15 tC/ha, respectively in order to reflect the larger release from stand replacing fires and the enhanced burning of organic soil material during high-fire years (*Goldammer et al.,* 2004; *Soja et al.,* 2004). In this manner, our inventory yields total carbon emissions for the Russian Federation and Mongolia ranging from 16 to 292 TgC/year (minimum in 1974, maximum in 1998) with an average value of 63 TgC/year. *Kasischke et al.* (2005) estimate emission fluxes of total carbon between 7.4 and 28 tC/ha for Russian boreal forest fires. For a range of burned areas between 2 and 14 Mha, this would yield annual carbon emission fluxes between 14.8 and 392 TgC/year, which is in reasonable agreement with our estimates, although our maximum emissions are 30% lower. *Soja et al.* (2004) estimated between 116 TgC for the year 1999 and 520 TgC for 2002 based on carbon consumption ranging from 3.4 to 75.4 tC/ha. Using their standard scenario (up to 5 cm of organic soil layer consumed by the fires), their estimates for the years 1998-2000 are 297, 173, and 257 TgC, respectively, compared to 292, 53, and 102 TgC in our inventory. We note that our estimates of average carbon consumption may be somewhat high biased. Using the fire radiative power method *Roberts et al.,* (2005) which provides a direct estimate of fuel (and thus carbon) consumption, *Wooster and Zhang,* (2004) found that "per unit area burnt, the results suggest Russian fires may burn less fuel and emit fewer products to the atmosphere than do those in North America." On the other hand we may underestimate the carbon consumption in extreme fire events, because our "crown fire" value of 25 tC/ha is only about one third of the maximum carbon consumption estimated by *Soja et al.,* (2004).

The seasonality of Russian fires (*Sukhinin et al.,* 2004) is less regular compared to the situation in North America. In some years, peak fire activity occurs in April or May, when the weather is dry and cold, and fires which are used for managing pastures get out of control. In other years,

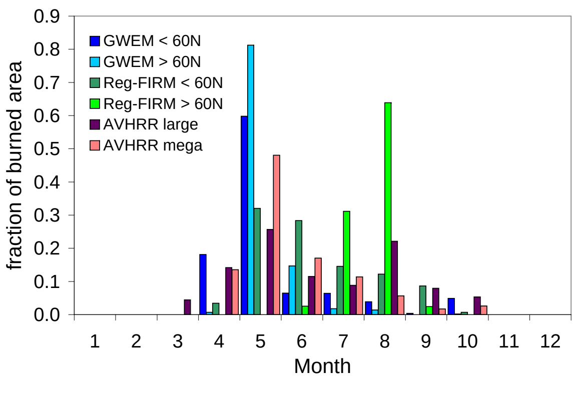

Figure 4. Seasonality of Russian fires south and north of 60°N based on GWEM 1.4 for the year 2000 and average values from Reg-FIRM. Note that unlike in North America, Russian fires do not necessarily follow a repeated annual pattern

the strongest fires occur in June or July, when a large fraction of fires is ignited by lightning strikes. Later in the season, fires are again predominantly of anthropogenic origin, i.e. as camp fires or for hunting purposes. According to *Goldammer et al.* (2004) illegal logging is another important reason for fires in Russia (particularly in Eastern Siberia) and Mongolia.

Figure 4 displays the seasonality of Russian fires according to Reg-FIRM (multi-annual average) and GWEM (year 2000). GWEM (i.e. GBA 2000) exhibits a strong maximum in May for fires north of 60°N, and a rapid drop off afterwards. Reg-FIRM also peaks in May, but the decrease in burned area is much slower. South of 60°N, GWEM also reports maximum burned area in May, whereas Reg-FIRM produces its peak in August. Based on a multi-year analysis of AVHRR fire counts (*Kasischke et al.,* 2005), some justification can be found for both of these patterns, although it is difficult to reconcile them quantitatively. In the *Kasischke et al.* (2005) study, a pronounced maximum is found in May for the extreme fire year 2003. Other years with relatively large fire activity exhibit a double peak, somewhat similar to the pattern simulated by Reg-FIRM. It may be that GBA 2000 experiences problems with detecting burned areas at the boundaries between snow covered and snow free regions. Changes between vegetated and barren surfaces may also play a role. In contrast, the active fire data reported by *Kasischke et al.* (2005) do not allow a quantiative comparison with burned area estimates and may lead to some seasonal bias if the ratio of fire counts and burned area changes with time. Based on this analysis we decided to apply the seasonality of Reg-FIRM for our inventory. We note that this will generate a seasonal pattern which is more regular than in reality. In order to obtain better quantitative estimates on Russian fire emissions in the future it would be highly desirable to compile a large fire data base for Central Asia based on a careful evaluation of different remote sensing products and including detailed latitude, longitude, and time information on individual fires of significant size.

4.3. Europe

In Europe, the dominant fire region is the Mediterranean region with Spain, Portugal, Italy, France and Greece as main contributors. Fires also occur in the northern part of Europe where the largest burned areas can be found in Poland and the Scandinavian countries. Due to higher biomass loads, these fires may be relatively strong emitters in spite of their smaller areas. National statistics of burned area after 1987 can be found in the ECE/TIM bulletins (UNECE/FAO publications, 2004, available via the Global Fire Monitoring Center http://www.gfmc.org/). According to these data the total burned area in Europe ranges from 285,000 ha in year 1996 to 911,000 ha in year 2000 with typically more than 90% occuring south of the Alps. More recent information on fires in Europe is also available from the European Fire Information System (http://effis.jrc.it).

Compared to emissions from fossil fuel burning, fire emissions in Europe are marginal. Even if we were to assume a rather carbon consumption per unit area of 30 tC/ha for all fires on the European continent, the total direct carbon emissions would reach only about 10% of the CO_2 emissions from Germany alone. CO and NO_x emissions are dominated by the residential, traffic, and power generation sectors, and fires will generally contribute less than 2% to the country totals for these species. A possible exception may be Poland, where fires could reach 5-10% of national CO emissions.

In order to estimate fire emissions for the past 40 years in Europe, we aggregated the ECE/TIM data into 18 regions and prescribed the reported burned area data after 1987. For earlier years, we used the average of the reported data and added some noise with 30% variability (Figure 5). Carbon consumption was set to 20 tC/ha for regions north of 48°N, and to 5 tC/ha for regions south of this latitude. For simplicity, all fires were treated as forest fires, even though the ECE/TIM bulletins report an almost equal fraction of shrubland fires and label a lot of the burned area as "other land". The seasonality is derived from qualitative information (International Forest Fire News, IFFN) and set to fractions of 0.02, 0.1, 0.35, 0.35, 0.15, 0.03 for the months from May through October, respectively. Based on these parameters, European fire emissions range from 1.32 TgC/year (1963) to 5.31 TgC/year (2000) with an average value of 2.56 TgC/year. This is in reasonable agreement with the estimate of about 4 TgC/year by *Kasischke et al.* (2005). We note that the approach used here explicitly excludes an analysis of possible trends in European fire activity. Such analysis would have to be performed in a separate study. This neglect is acceptable for the present study, because of the minor importance of fires for emissions in Europe between 1960 and 2000.

5. RETRO inventory parameters for tropical and subtropical forest and savanna fires

Fires in tropical and subtropical regions are predominantly anthropogenic in nature, although lightning-induced fires do occur regularly and have a long history, which led to the development of fire-resistent trees and bushes throughout large parts of Africa, South America, Southeast Asia, and Australia (e.g. *Mueller-Dombois and Goldammer,* 1990). Savannas generally contribute most to the annual area burned of the tropics and sub tropics, but in terms of emissions, tropical forest fires may have become equally important over time. In spite of the importance of tropical fires, there is still a huge deficit in quantitative information on burned areas, fuel loads, and fire characteristics, and the situation is particularly dire for the time before the mid-1990s, when satellite data became available to help identifying the dominant burning patterns and their seasonal cycle.

In contrast to the boreal and temperate regions, tropical and subtropical fires are far more numerous and can be better described statistically for building this inventory. Due to increasing anthropogenic influence, landscapes are often highly fragmented, and this makes it very difficult to obtain reliable quantification of fire emissions from space. Recent

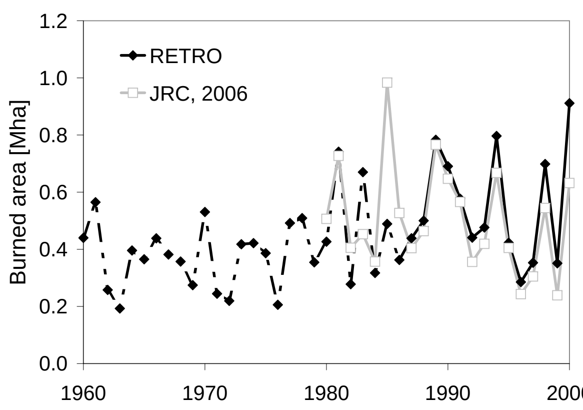

Figure 5. European burned areas used in the RETRO inventory. Data after 1987 from the ECE/TIM bulletins, earlier values are averages with added random noise. The data are compared with recent estimates from JRC, Ispra (personal communication, 2006) which cover the time period 1980–2000

estimates on tropical fire emissions differ by at least a factor of two, and if uncertainties are properly evaluated, they are even larger than this (e.g. *Robinson,* 1989). Unfortunately, at present even the constraints from inverse modelling techniques do not allow for a more accurate description of tropical fire emissions. This is discussed in the main part of this paper.

In relation to the uncertainties of present-day emissions from tropical fires, it is even more difficult to establish reliable trend estimates over the past 40 years. There are two competing factors, and it is unclear which of them is more important: on the one hand, population density, and thus anthropogenic pressure has increased tremendously during the past decades, on the other hand, this also increased the fraction of managed land, and therefore might have led to decreased fuel loads and reduced average fire size.

5.1. Africa

The African continent is undoubtedly the continent with the most pronounced fire activity (e.g. *Andreae,* 1991; *Dwyer et al.,* 2000). Monsoonal rains, pronounced dry seasons, and increasingly large human pressure are the major reasons for frequent fires destroying about half of the widespread savanna regions in Africa each year. Fires occur almost any time of the year, but there are two distinct peak fire seasons with maximum activity in the Northern hemisphere (NH) in December and January and in the Southern hemisphere (SH) in July and August.

Table 5 lists a number of burned area estimates from the recent literature. Some studies suggest that the burned area is somewhat larger in the NH, but due to higher fuel loads, the SH dominates the emissions. However, given the large uncertainties associated with these estimates, this statement may be challenged when improved data sets become available. The total area burned estimates vary by a factor of four (from 121 to 547 Mha/year) between different studies. The results from the World Fire Atlas are much lower than all other studies, which is due to the fact that this product is based on nighttime observations when fire activity is low.

Estimates based on fire counts (hot pixels) tend to be larger than those derived from burned scar mapping, which might be attributed to the frequency of small fires throughout large areas of fractionated landscapes in Africa and is furthermore a result of the lower threshold for active fire detection (less than 10% of the pixel size) compared to burned scar detection (about 40% of the pixel size, H.D. Eva, personal communication, 2004). It is difficult to differentiate between small savanna fires and agricultural fires unless very high resolution imagery (e.g. from Landsat) is used (H.D. Eva, personal communication, 2004).

5.1.1. Savanna fires

The majority of African wild fires are savanna and woodland fires. The interannual variability of the burned area appears to be relatively small in the NH, but can be significant in the SH. *Barbosa et al.* (1999) find a variability of 15% in the former and up to a factor of three in the latter. In contrast, the burned area estimates from *van der Werf et al.* (2004) also vary by about 15% in the NH, but only by 10% in the SH (G. van der Werf, personal communication, 2005). The revised data in version 2 of the GFED inventory (*van der Werf et al.,* 2006) show the same variability in the northern hemisphere, but only about 30 % variablity in the southern hemispheric part of the continent. The Reg-FIRM model produces a reasonable geographical and seasonal distribution of burned area (Figure 6), but the absolute amounts are lower than the satellite-based estimates listed in Table 5. The interannual variability of Reg-FIRM is about 40 % in the northern hemisphere and a factor of two in the southern hemisphere.Reg-FIRM burned areas show no significant correlation with the ENSO 3.4 index. In contrast to the results obtained by *Barbosa et al.* (1999), Reg-FIRM burned areas in SH Africa for the El Niño year 1987 are higher than for the surrounding years (Figure 6).

There are many different woodland and savanna ecosystems in Africa, and their fuel load and burning behaviour differ significantly (*Barbosa et al.,* 1999). Often, the fuel load exhibits large inter-annual variability (e.g. *Anyamba et al.,* 2003), which can influence fire spread, and thus the burned area, and ultimately the emissions from African savanna fires. In our inventory this effect is partially accounted for inasmuch the Reg-FIRM model does include variations in the fuel load in order to calculate the burned area. However, if there is an amplifying or compensating effect of fuel load with respect to burning efficiency and completeness, then this is not represented in our inventory and we may therefore underestimate or overestimate the variability of savanna fires. Clearly, further validation of the Reg-FIRM model for the African continent would be valuable here.

Generally, the biomass density of African biomes is relatively low: *Barbosa et al.* (1999) give values between 1 and 8 t/ha. Assuming a carbon content of 50% and complete combustion, this implies maximum net carbon emissions of 4 tC/ha. *Ito and Penner* (2004) list average values of 2.9 and 1.4 tC/ha for woodlands and grasslands, respectively, while *Hoelzemann et al.* (2004) used values of 7.5 and 1.5 tC/ha.

Previous studies estimated the total direct carbon emissions from fires on the African continent between 432 and 1702 TgC/year (Table 6). Most estimates fall in the range of 800 to 1000 TgC/year, and we use this as a target value for the long-term average emissions from African savanna and grassland fires in our inventory. Burned areas are taken from the Reg-FIRM model and are scaled by a factor of 2 in order to yield estimates closer to the literature values. The resulting average burned areas are 136 (88–199) Mha/year and 133 (71–291) Mha/year for NH Africa and SH Africa, respectively. This is consistent with the values from GBA2000 and GFED, but almost a factor of two lower than the estimates by *Barbosa et al.* (1999). In both hemispheres we assume 60% of fires occur in wooded ecosystems, and 40% in grasslands. Carbon consumption is set to 1.5 tC/ha for grasslands, and 4 and 5 tC/ha for wooded areas in the NH and SH, respectively. Based on a reviewer comment we note that the latter value is likely overestimated by 20–40 %.

5.1.2. Deforestation fires

In the European TREES project (Tropical Ecosystem Environment Observation by Satellite) tropical deforestation rates were estimated to account for about 0.85 Mha/year forest loss in the primary forest area in Africa to which another 1.5 Mha/year must be added for deforestation outside this domain (*Achard et al.,* 2004). *Houghton* (2003) state somewhat larger estimates of 5.52 Mha/year. Even if all of this would be counted as burned area it would still constitute only a minor fraction of African fires. However, because of much higher amounts of fuel consumed (a factor of 5-20 more than in savannas), the emissions from African forest fires are significant (probably 10-20% of the total carbon emissions). Tropical forest fire net carbon emissions are estimated as 24 tC/ha by *Ito and Penner* (2004) and 36 tC/ha by *Hoelzemann et al.* (2004). *Achard et al.* (2004) derive net emissions of 27 tC/ha (20 % combustion efficiency applied to 143 tC/ha fuel load) for the primary tropical forest and 7 tC/ha for secondary forest (20 % of 36 tC/ha). *Houghton* (2005) gives a fuel load of 110 tC/ha for primary forests and less than 100 tC/ha for secondary

Table 5. Comparison of burned areas from African fires

Burned area [Mha] 1997	1998	1999	2000	other	Comments	Reference
Whole continent						
222	233	221	230		GFED-2	*van der Werf et al.*, 2006
262	306	334	321	270 (179-450)[a]	Reg-FIRM with linear scaling	this study
			227		GBA2000	*Boschetti et al.*, 2004
			121		GLOBSCAR	*Boschetti et al.*, 2004
			2.3		World Fire Atlas	*Boschetti et al.*, 2004
				547 (359-687)[b]	AVHRR fire counts	*Barbosa et al.*, 1999
Northern hemisphere						
157	136	149	153		GFED-2	*van der Werf et al.*, 2006
161	135	166	194	136 (88-199)[a,d]	Reg-FIRM with linear scaling	this study
			126		GWEM 1.4	*Hoelzemann* (2006)
				362 (304-391)[b]	AVHRR fire counts	*Barbosa et al.*, 1999
				167[e]	TRMM-VIRS fire counts	*van der Werf et al.*, 2003
Southern hemisphere						
65	98	73	76		GFED-2	*van der Werf et al.*, 2006
300	240	240	230	225 (180-300)[b]	MODIS burnt area	*Ito et al.*, 2007
102	171	168	127	133 (71-291)[a]	Reg-FIRM with linear ascaling	this study
			111		GWEM 1.4	*Hoelzemann* (2006)
			108		GBA 2000	*Palacios-Orueta et al.* (2004)
				185 (54-297)[b]	AVHRR fire counts	*Barbosa et al.*, 1999
				116[e]	TRMM-VIRS fire counts	*van der Werf et al.*, 2003
				399	climatology (1980s ?)	*Scholes et al.*, 1996

[a] average and range for years 1960-2000
[b] average and range for years 1981-83 and 1985-91
[c] average and range for years 1998-2005
[d] northern hemisphere includes all tropical deforestation
[e] average for years 1998-2001

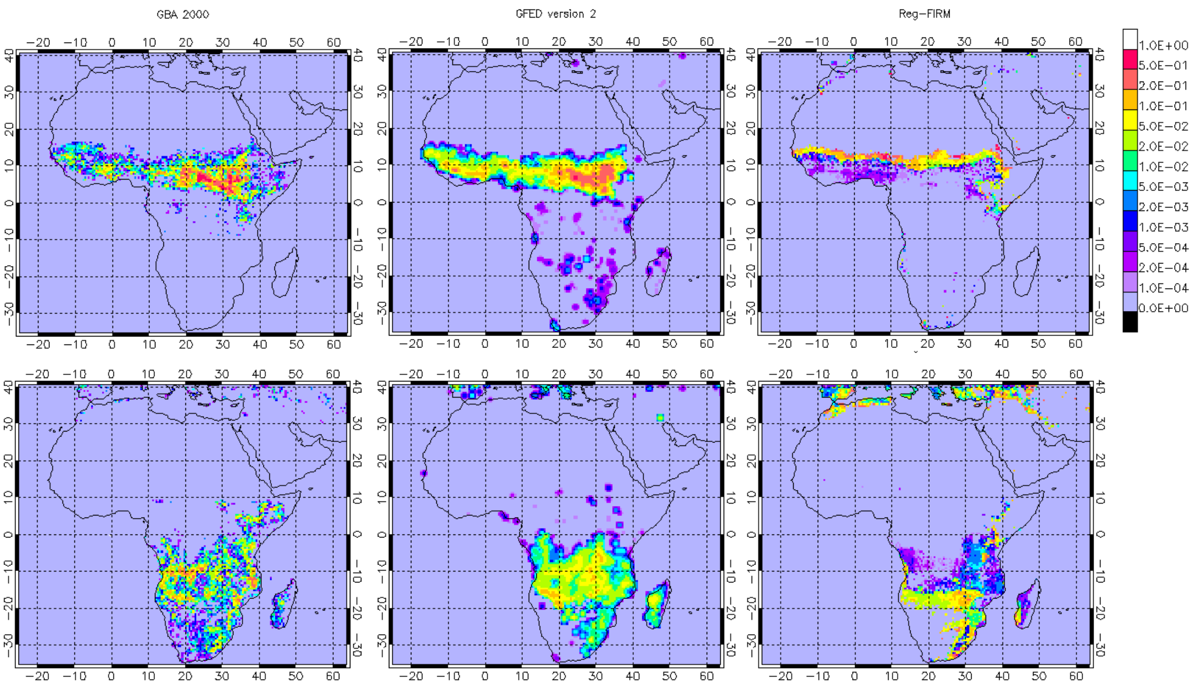

Figure 6. Comparison of burned fractions in Africa for January and August 2000.

forests in Africa. Assuming an emitted fraction of 33 %, this would yield net carbon emissions of 36 tC/ha as assumed by *Hoelzemann et al.* (2004).

For the RETRO inventory we adopted the burned area estimates by *Houghton* (2003) and used fuel load estimates from *Achard et al.* (2004) together with a burning efficiency of 0.33 according to *Ito and Penner* (2004). Tropical deforestation fires are added to the inventory using a linearly increasing deforestation rate with no burning in the year 1950 and the *Houghton* (2003) value of 5.52 Mha/year in the year 2000. The net carbon emissions for deforestation fires are 25 tC/ha, which is a weighted average of the biomass loads in the TREES and non-TREES areas given by *Achard et al.* (2004) multiplied with a constant factor of 0.33 to describe the fraction of carbon released during the burn.

5.1.3. Emissions, spatial distribution and seasonality

Table 6. Comparison of total carbon emissions by African fires

Year	Carbon emissions [tC/year]	Reference
1960-2000	669-1678	this study
1985/86, 1987-91	432-861	*Barbosa et al.,* 1999
1980-2000	887	*Duncan et al.,* 2003
1997-2000	1030	*van der Werf et al.,* 2003
1997-2000	1138-1283	*van der Werf et al.,* 2006
1997-2000	988-1247	this study
2000	932	*Ito and Penner,* 2004
2000	891	*Hoelzemann et al.,* 2004
2000	1558	*Palacios-Orueta et al.,* 2004
2000	1181	this study

The resulting carbon emissions from fires in Africa range from 669 TgC/year for the year 1961 to 1678 TgC/year for the year 1992 with an average of 992 TgC/year. Fire emissions from the southern hemispheric part of the continent are on average equal to emissions in the northern hemisphere: the SH/total ratio varies from 35 % to 64 %. For the year 2000, *Palacios-Orueta et al.* (2004) find an SH/total ratio of 63 %. Recent remote sensing data of fire radiative energy (*Roberts et al.,* 2005; *Wooster et al.,* 2005) indicate that the notion of approximately equal carbon emissions from both hemispheres is correct (M. Wooster, personal communication 2007). However, up to now there are too little data to reliably assess the inter-annual variability of this ratio. Table 6 compares total direct carbon emission estimates from several recent studies with the values from our inventory. The results for the years 1998–2000 are generally in good agreement with the estimates from version 2 of the GFED inventory by *van der Werf et al.* (2006). The inventories based on the GBA 2000 burned area data set (*Hoelzemann et al.,* 2004; *Ito and Penner,* 2004) generally yield somewhat lower estimates. Likewise, the estimates by *Barbosa et al.* (1999) and *Duncan et al.* (2003) are lower by about 30 % compared to our results. We note that *Duncan et al.* (2003) did not apply their scaling methodology using the variability of the TOMS aerosol index to African fire emissions. Their value thus constitutes a climatological average. One study (*Palacios-Orueta et al.* (2004)) finds carbon emissions which are higher by about 30 %.

The spatial distribution and seasonality of woodland and grassland fires in the RETRO inventory is taken from the GWEM 1.4 model results, while deforestation fires are distributed randomly across the deforestation areas identified in the TREES project .

We analyzed results from the GFED inventory version 2 to investigate the relative roles of burned area and fuel load variability for fire emissions in Africa. Figure 8 shows excellent correlation between carbon emissions and burned area for both, southern Africa and the Sahel region. These are two regions where one might expect a strong influence of varying fuel loads (cf. *Barbosa et al,* 1999). For South Africa we find a weak negative correlation ($r^2 = 0.23$) of GFED2 carbon emissions with fuel load, while in the Sahel, this correlation is positive with $r^2 = 0.75$. These results support our claim that the interannual variability of fire emissions can generally be well represented by the variability in burned area. However, we note that GFED2 uses a model to estimate fuel load variability and could potentially underestimate this quantity.

5.2. South America

There has been considerable research into the amount and distribution of fires in South America (here defined as south of the equator) in recent years. Yet, large uncertainties remain and little is known about the interannual variability or possible trends in these fires. While deforestation of primary forests has received most attention in the news and in the scientific literature, most fires in South America occur just outside the primary forest in areas undergoing rapid land-cover conversion to cattle ranching and broad-acre cropping (*Potter et al.,* 2002, *Cardoso et al,* 2003; *Cochrane,* 2003). *Achard et al.* (2002) give an average deforestation rate of 2.2 Mha/year for the time period 1990 to 1997, and they state that the deforestation rate in South America has remained relatively constant after 1980. In a revised estimate *Achard et al.* (2004) give somewhat higher deforestation rates for Amazonia totaling 3.3 Mha/year (1.08 Mha/year within the TREES domain, and 1.9 Mha/year outside of this region). Given the fact, that Brazil constitutes the major fraction of land area and burning activity in Amazonia, these numbers appear consistent with deforestation data collected by the Brazilian National Institute for Space Research (INPE), who report deforested areas between 1.1 and 2.9 Mha/year in the time period of 1977 to 2002 with no apparent trend. The estimate of *Houghton* (2003) is larger: they estimate a deforestation area of 7.4 Mha/year for "tropical America" during the 1980s and a decline to 4.55 Mha/year during the 1990s.

The burned areas of recent satellite products range from about 12 to 21 Mha and mostly describe fires outside the tropical forest. The Reg-FIRM model simulates somewhat larger burned areas (41-year average: 28 Mha). It predicts a large region of intense burning in the Chaco subtropical dry leaf forests of Argentina, which is much less emphasized in the satellite fire products.

There are large differences in the carbon emission estimates from South American fires between different studies. *Potter et al.* (2002) and *van der Werf et al.* (2004) mark the upper end of estimates with 800 TgC/year (710 TgC/year for Brazil), while the lower end is given by inventories based on the GLOBSCAR or GBA 2000 burned area data sets (Table 7). *Potter et al.* (2002) note a close agreement with the statistical inventory of *Hao and Liu* (1994), which was however based on very little quantitative information (W.N. Hao, personal communication, 2001). A recent intercomparison of chemistry transport model results using different vegetation fire inventories with CO data from the MOPITT instrument indicates a better agreement with the higher emission estimates (*Hoelzemann,* 2006). However, as noted by *Petron et al.* (2004), considerable uncertainties remain when MOPITT data are used to infer emission estimates.

Due to the extremly large uncertainties of fire emissions in this region, any choice of parameters will be somewhat arbitrary. We adopt an estimate of 35 tC/ha for the tropical forests based on the fuel loads given by *Achard et al.* (2004), who report an average biomass of 186 and 47 tC/ha for forests in the TREES domain and outside this domain, respectively. The combustion completeness is assumed to be 33 % as in *Ito and Penner* (2004). For comparison, *Houghton* (2005) reports a fuel load of 130 tC/ha for tropical America. For secondary forests/woodlands (80%, classified as "wooded" in our inventory) and cerrado savannas

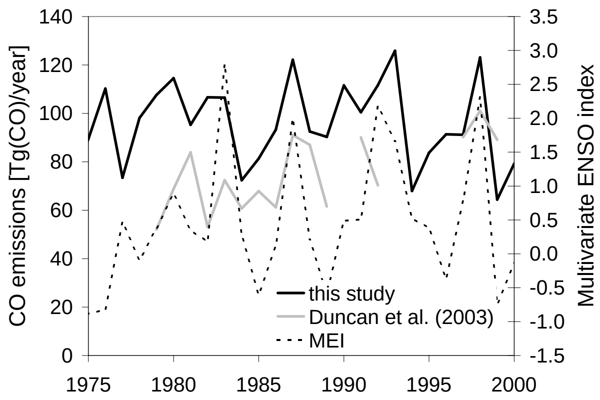

Figure 7. Interannual variability of CO emissions from South America in comparison with re-computed values of *Duncan et al.* (2003) and the Multivariate ENSO index for the months of April and May

(20%, classified as "grass"), we apply carbon consumption values of 20 tC/ha and 2 tC/ha, respectively. Deforestation rates are assumed to increase linearily after 1950 up to a total of 5.92 Mha/year in the year 1985. This value is 80 % of the estimate by *Houghton* (2003) for the whole tropical America region in the 1980s. Between 1985 and 1995 we decrease the deforestation rate to 3.64 Mha/year where it remains until the year 2000. The interannual variability of burned areas outside the primary forests is derived from the Reg-FIRM model in the latitude band 20°S to the equator. The Reg-FIRM burned areas are distributed across the whole South American continent in order to be consistent with the satellite observations outside the primary forest regions. These parameters yield total carbon emissions between 340 and 808 TgC/year (minimum in 1964, maximum in 1993) with a mean value of 548 TgC/year.

Interestingly, owing to a large burned area estimate of 42 Mha, the 1993 value of our inventory agrees very well with the estimate of 800 TgC/year of *Potter et al.* (2002), who also investigated the 1992/1993 fire season (Table 7). Our average estimate for the late 1990s lies in between the inversion study by *van der Werf et al.* (2004) based on version 1 of the GFED inventory and the forward modeling results of GFED version 2 (*van der Werf et al.,* 2006). The interannual variability pattern agrees better with *van der Werf et al.* (2004) than with the more recent study, although there is a large discrepancy for the year 1999.

In Figure 7 we compare our CO emission estimates for the years 1975-2000 with re-computed values following the *Duncan et al.* (2003) methodology of using the TOMS aerosol index to obtain the interannual variability of the emissions. Generally, the magnitude of variability seems in good agreement. The two inventories agree on marking the years 1987 and 1998 as high fire years, but there are obvious differences for other years (e.g. 1986 and 1996). Also shown in this Figure 7 is the multivariate ENSO index (J. Null, http://www.ggweather.com/enso/years.htm) for the months of April and May. Although there appears to be some common variance between the data sets, the overall correlation remains poor ($r^2 = 0.1$) and is even smaller for other months of the ENSO index.

5.3. Central America

Fires in Central America have received little attention in the global fire modelling community compared to the situation in South America, Africa, or Indonesia. An exception were the very large forest fires associated with the El Niño in 1998, which caused severe smog over a period of three months. *Cochrane* (2002) has compiled burned area estimates from different sources and notes that in 1998 almost 3 Mha of predominantly forested land were burned. The GWEM 1.4 inventory reports a burned area of 2.4 Mha for the year 2000, while the GFED version 2 inventory lists values between 1.6 Mha for the year 1997 and 9.8 Mha for 1998.

Much of the land in Central America is tropical forest which does not burn naturally. The forest fires observed in this region originate either directly or indirectly from deforestation (*Cochrane,* 2002). Primary forests are logged and the logs are left to dry until they can be burned with little residue. There may be regrowth of forest some years later, but this secondary forest has very different properties (e.g. much higher fuel loads) and is much more susceptible to burning. It is probably safe to assume that most of the fire emissions in Central America, and in particular most fires in 1998, originate from such secondary forest burning.

Due to the lack of more detailed information we have to make several assumptions in prescribing the fire emissions

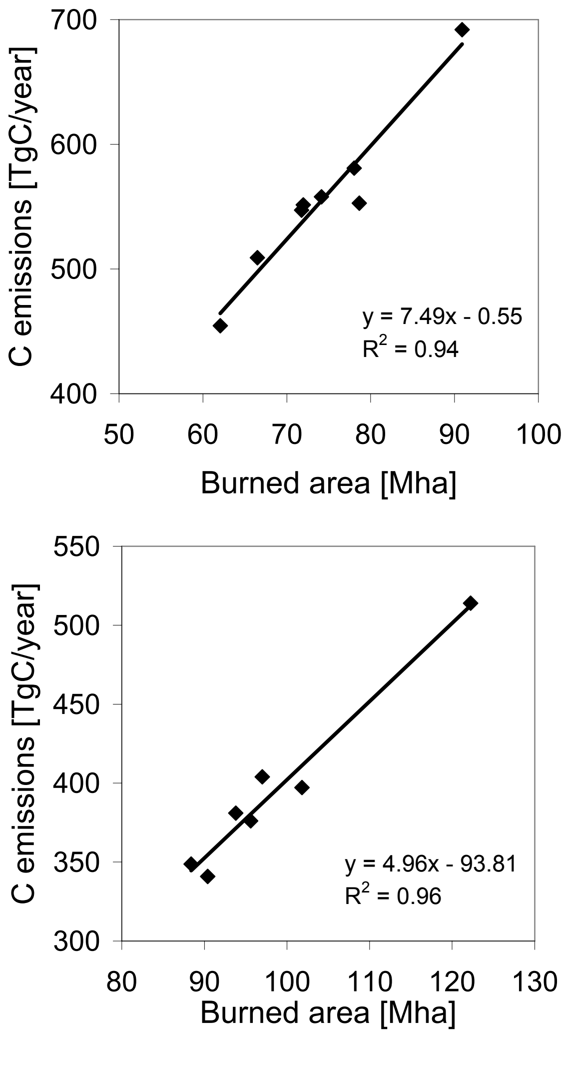

Figure 8. Correlation between burned area and total carbon emissions for South Africa (top) and the Sahel zone (bottom) in the GFED inventory version 2 (*van der Werf et al.,* 2006). Each symbol represents a regional annual average value.

Table 7. Comparison of total carbon emissions from South American fires for the late 1990s

Carbon emissions [TgC/year]					Comments	Reference
1997	1998	1999	2000	2001		
			87		based on GLOBSCAR	*Hoelzemann et al.,* 2004
			90		based on GBA 2000	*Ito and Penner,* 2004
750					1990s average	*Houghton,* 2003
800					1992/93 fire season	*Potter et al.,* 2002
780	920	770	480	610	Inversion results	*van der Werf et al.,* 2004
304	397	370	189	278	GFED version 2	*van der Werf et al.,* 2006
561	779	363	484		this study	

in Central America between 1960 and 2000. For deforestation rates we use the same parameterisation as in South America, assuming that 20 % of the Latin American deforestation rates given by *Houghton* (2003) apply to Central America. Burned areas for other vegetation are obtained from the Reg-FIRM model. In order to reproduce the strong enhancement of burned area in the year 1998, we apply a special scale factor here. The resulting average burned area in Central America is 1.37 Mha/year. The average over the 1990s is 1.96 Mha/year, and for 1998 we estimate a burned area of 3.15 Mha.

The net carbon emissions are set to 43 tC/ha, which is 33% of the biomass estimate of 129 tC/ha by *Achard et al.* (2004). All fires are attributed to forested land. The resulting emissions range from 13 TgC/year (1966) to 135 TgC/year in 1998 with an average of 59 TgC/year. Figure 9 shows a comparison of the CO emissions resulting from our parameterisation with the values obtained by *Duncan et al.* (2003) using the TOMS aerosol index to describe the interannual variability. The agreement between the two data sets is quite good and better than in other world regions. *Duncan et al.* (2003) produce a somewhat stronger enhancement for the fires in 1998 in agreement with the analysis of *Rogers and Bowman* (2001) who also used the TOMS AI as indicator and found an enhancement of a factor of 2-3 for 1998 compared to the climatological average.

5.4. India

India is treated separately in this study, because of its extremely high proportion of agricultural land, which limits the applicability of the Reg-FIRM model and mandates a careful screening of satellite-derived burned areas for distinguishing agricultural from wildland fires (within the RETRO inventories, agricultural fires are subsumed under anthropogenic activities).

The GBA2000 data set (*Tansey et al.,* 2004) reports a total area burned of 6.6 Mha for the complete South Asia region of which 4.3 Mha originate from wooded ecosystems in India. This value is broadly consistent with the officially reported burned area of 3.7 Mha for Indian forests (*Bahugana and Singh,* 2002). The Reg-FIRM model produces considerably larger burned areas on the Indian sub continent (almost 20 Mha/year on average). However, this model describes fires under natural vegetation conditions whereas the majority of the Indian land surface is cultivated land.

GWEM 1.4 and GFED yield relatively similar estimates for fire emissions in India for the year 2000: GWEM 1.4 reports a total of 7 TgC/year, whereas GFED produces 5.2 TgC in 2000 and ranges from 5.2 to 8.9 TgC/year in the 5-year period 1997-2001 (with lower emissions in 2000 and 2001). These values are difficult to reconcile with the burned area estimates if we assume average net emissions of 10–30 tC/ha for forests as in other world regions. For lack of better knowledge we adopt the GWEM 1.4 emission fluxes as target values and adjust the Reg-FIRM burned areas and the ecosystem specific carbon consumption values accordingly. This leads to rather low carbon consumption of 2.5 tC/ha for grid cells dominated by forests and 1.5 tC/ha for shrubland cells. Reg-FIRM burned area results are scaled with a factor of 0.15.

5.5. Southeast Asia

For the purpose of this study we define South East Asia as the region comprising of Myanmar, Laos, Vietnam, Cambodia, Bangladesh, and Southern China. Indian and Indonesian fires were treated separately (see previous and following sub sections). Most of the fires in South East Asia occur in the subtropical forests of Myanmar, Cambodia, and Thailand from January through April. There are indications that many fires in these regions involve peat burning associated with deforestation, but only little reliable information is available.

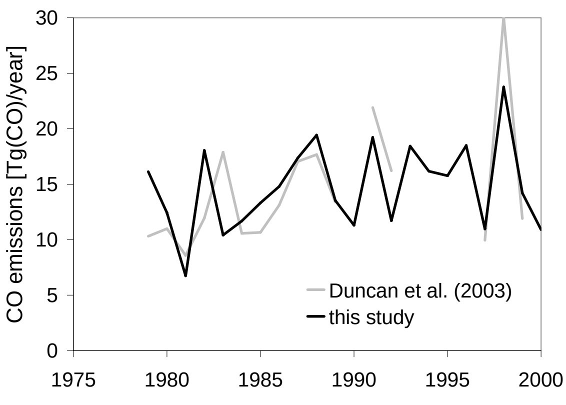

Figure 9. Interannual variability of CO emissions from Central America in comparison with re-computed values of *Duncan et al.* (2003)

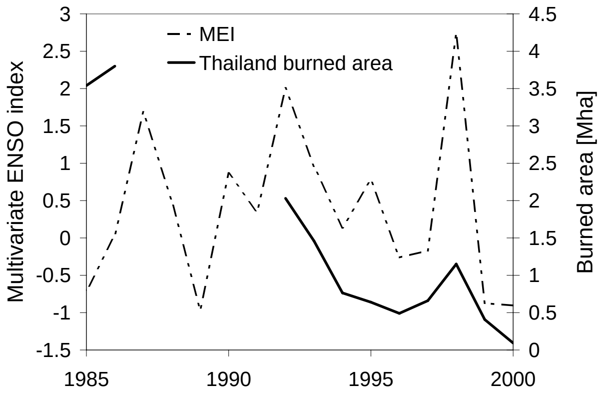

Figure 10. Multivariate ENSO index for February and March and annual burned area in Thailand as reported in IFFN (2001)

Information on deforestation rates is sparse. The main data sources are the paper by *Achard et al.* (2004), and the International Forest Fire News (IFFN). *Achard et al.* (2004) give a total annual South East Asian deforestation rate of 2.84 Mha/yr. This estimate includes Indonesia. On a web site of the TREES project (http://www-gvm.jrc.it/Forest/Asia/hotspots.htm), the authors differentiate between continental South East Asia and the islands and find that about 40% of the burned area is on the continent. The IFFN provide some country-level information, which is however mostly limited to estimates of forest cover between two years (for example 1973 and 1991). Only Thailand reported annual burned area estimates for 1985, 1986 and 1992-2000. We correlated these data with the Multivariate ENSO index for February and March and found a correlation coefficient r^2 of 0.63. On average, fires in Thailand account for about half of the burned area in continental South East Asia if we assume that the average annual rates derived from the sparse information for other countries are applicable for the 1990s. For our inventory we estimate the deforestation rates as twice the value calculated for Thailand from the linear correlation with the ENSO index, and we limit the minimum value to 10^5 ha (Figure 10). The maximum value thus obtained is 3.8 Mha in the year 1983, and the mean value over the period 1990 to 1997 is 1.88 Mha, which is 65% larger than the estimate of 1.14 Mha by *Achard et al.* (2004) and amounts to about 75 % of the average annual deforestation rate for tropical Asia given by *Houghton* (2003).

There are indications that deforestation rates in South East Asia have significantly increased in the most recent years, possibly due to increased demand for timber in China and perhaps associated with the economic slowdown in the region after 1997. This trend is not reflected in the correlation of the Thailand burned areas with the ENSO index. In order to account for this recent trend we disregard the burned area values obtained from the ENSO correlation after 1998 and instead add 10 % and 20 % to the 1998 value for 1999 and 2000, respectively. These factors are based on information from the GFED version 1 inventory (*van der Werf et al.,* 2003) which yields a steady increase of emissions from 115 to 270 TgC/year during the period 1997-2001.

February and March of 1998 exhibit a very strong positive ENSO index and thus yield burned area estimates which are almost a factor of three larger than those for the year 1997. On the other hand, February and March 1999 and 2000 have a relatively strong La Niña signature and would therefore lead to rather low burned area estimates. A potentially important factor which is not accounted for in our inventory is the second war in Indochine (aka Vietnam war). Reportedly, this war led to widespread deforestation in Laos and Vietnam (these countries lost 23% and 12% of their total forest area between 1960 and 1972, respectively). Not all of this deforestation was associated with fires, however, so that emissions from burning may have been similar to those from later years when economic use of the forests increased substantially.

According to *Achard et al.* (2004), the Southeast Asian forest biomass averages at 152 tC/ha, and 20% of this is released during the burning of a forest. This would yield net average carbon emissions of 30 tC/ha, which is near the upper end of estimates for other tropical forests (e.g. *Ito and Penner,* 2004). We adopt this parameter and assume that it accounts for some fraction of the fires being associated with peat burning. This results in average carbon emissions from Southeast Asian forest fires of 45 TgC/year. The year 2000 estimate is 116 TgC/year, which is somewhat larger than the GWEM 1.4 estimate (73 TgC/year), and significantly lower than the GFED version 1 estimate (240 TgC/year), but in excellent agreement with the GFED version 2 value of 108 TgC/year.

Heald et al. (2003) estimate Southeast Asian fire emissions of CO for spring 2001 based on the inventory of *Duncan et al.* (2003) with corrections based on daily AVHRR fire observations. They give a total of 69.3 Tg(CO) for a region somewhat larger than what is defined as Southeast Asia in this study. However, an inverse modelling analysis by the same authors (*Heald et al.,* 2004) suggested that the actual value might be much smaller than this, because the total CO emissions estimate (including residential and industrial emissions) in a region similar to ours was reduced from 69 Tg(CO) (a priori) to 42 Tg(CO) (a posteriori), and fires contribute a large fraction of the total emissions there. Using the emission ratio for tropical forests from *Andreae and Merlet* (2001), our value for the year 2000 corresponds to about 27 Tg(CO). This appears to be broadly consistent with the a posteriori estimate of *Heald et al.* (2004), especially if we assume a generally increasing trend in fire activity in this region as suggested by *van der Werf et al.* (2006). Clearly, fire emissions in continental South East Asia deserve a lot more attention than they received up to now.

Very little is known about fire in other vegetation types in this region. Shrubs and grasslands are mostly present in the Himalaya region and in Southern China. In order to account for some fire emissions from wooded ecosystems and grasslands here, we prescribe a constant burned area of 100,000 ha, which is equally distributed among the wooded and grass fractions. Carbon consumption is set to 4 tC/ha and 1.5 tC/ha, respectively. These values yield annual emission fluxes of 0.2 TgC/year, which is much lower than the estimate of GWEM 1.4 of 11 TgC/year.

5.6. Indonesia

Fires in Indonesia are almost entirely a consequence of land conversion. The extreme smoke and haze produced during the 1997 and 1998 fires received much attention in the news media and in the scientific literature (c.f. *Page et al.,* 2002; *Heil et al.,* 2005). Indonesia has the largest reservoir of tropical peatlands. Large areas of eastern Sumatra, southern Borneo, and Irian Jaya are covered with peat soils which can reach depths of more than 10 m and a biomass density exceeding 7000 tC/ha (*Shimada et al.,* 2001). A significant fraction of these peatlands has been drained in order to allow for land conversion, and this has greatly exacerbated fire risk in Indonesia. There is a strong relationship between El Niño and the Indonesian fire activity, because the extreme drought during an El Niño year provides favorable conditions for clearing more land. At the same time the enhanced susceptibility of the vegetation under El Niño conditions increases the risk of large uncontrolled fires and sustained peat fires.

Due to the extremely large inter-annual variability of emissions from Indonesian fires, a different methodology was developed for this region. Burned areas and carbon emissions were calculated following the approach of *Heil et al.* (2005), who established scaling factors for fire counts from the Along-Track Scanning Radiometer (ATSR, *Arino et al.,* 1999) based on detailed burned area statistics available for the 1997/98 fire season (*Tacconi et al.,* 2003). The average burned area in forest landscapes (primary forest, fragmented forest and forest plantations) during the 1990s amounts to 0.45 Mha/year, while about 7 Mha of forest burned during the extreme fire season of 1997/98. Biomass loads and net carbon emissions per unit area were assigned to three different vegetation classes extracted from *Loveland et al.* (2000). For primary forests we used 504 tons dry matter per ha (TDM) and 98 tC/ha, respectively. Fragmented forests were assigned 200 TDM and 54 tC/ha, and for agricultural land, savanna, and grasslands we used values of 40

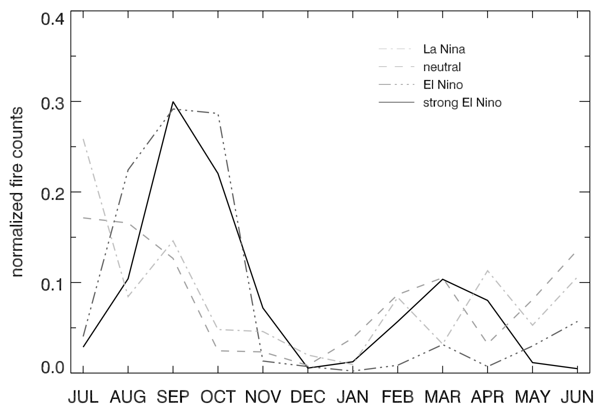

Figure 11. Seasonality of fires in Indonesia under different ENSO conditions, derived from ATSR fire count data

TDM and 19 tC/ha, respectively. The latter value is relatively large compared to other world regions because of the inclusion of plantations, which often consist of sugar canes. The distribution of peat soils was determined according to the FAO World Reference Base (WRB) for Soil Resources (*FAO,* 2003). For fires in areas with peat soils emissions of 352 tC/ha were added to the emission flux from the corresponding vegetation type. This value is consistent with an average peat burning depth of 0.5 m, which corresponds to the medium estimate of *Page et al.* (2002). Burned area estimates for years before the ATSR time series (i.e. prior to 1996) were extrapolated based on the multivariate ENSO index (average from October to March, *Wolter and Timlin,* 1998), which we found highly correlated ($r^2 = 0.93$) with the number of annual fire counts from the ATSR sensor between 1996 and 2003.

In order to account for the increasing trend in land conversion and forest vulnerability since the 1960's, we scaled the complete time series with the interpolated deforestation trend from *Holmes* (2002). A polynomial fit to these data yielded the following expression with a correlation coefficient of $r^2 = 0.97$:

$$A = 0.223 + 0.0137(y - y_{ref}) + 1.8 \times 10^{-4}(y - y_{ref})^2 \quad (2)$$

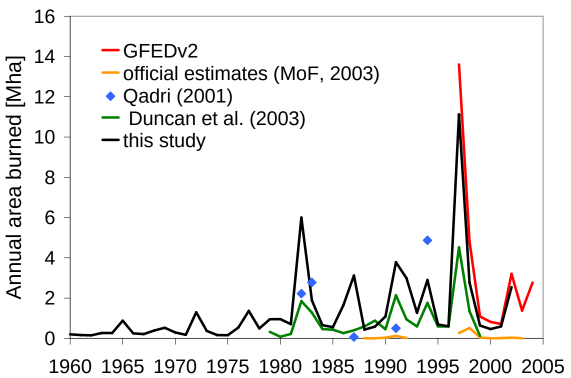

Figure 12. Interannual variability of burned areas in Indonesia in comparison with other estimates. Values labelled *Duncan et al.* (2003) were re-computed based on their TOMS AI scaling factors corrected for background aerosol and volcanic influence

where y denotes the calendar year and y_{ref} is the reference year (1960).

Because of the pronounced dependency of the seasonal and spatial distribution of Indonesian fires on the state of the Southern Oscillation (Figure 11), we developed four different monthly templates from the 1996-2003 ATSR time series. One template was then selected for each fire year (July-June). The distinction between strong and weak El Niño, neutral, and La Niña years was made according to the analysis of J. Null (http://www.ggweather.com/enso/years.htm).

This composite approach provides a relatively robust treatment of the extreme variability observed in Indonesian fires and captures in particular the strongly enhanced emissions during and after the 1982/83 and 1997/98 El Niño events, which were exacerbated by the unusual droughts in these years (*Toma et al.,* 2000). Figure 12 shows the temporal evolution of burned areas in comparison with the values from the GFED version 2 data set (*van der Werf et al.,* 2006), official estimates from the Indonesian forest ministry (*MoF,* 2003) and a few individual values taken from *Qadri* (2001). Also shown is the relative variation of emissions inferred from the TOMS aerosol index (*Duncan et al.,* 2003). Generally, our method appears to reproduce the variability and trend pattern quite well. Most noteworthy is probably the excellent agreement of the temporal pattern with the GFED version 2 estimates. There are indications that the *Duncan et al.* (2003) approach underestimates the extreme enhancement of emissions during the 1997/98 El Niño period, because it does not properly account for the burning of peat.

In spite of our efforts to consider the temporal trend in deforestation rates, the trend in emissions may be underestimated (i.e. emissions in early years may be overestimated), because we assume a constant depth of peat burning over time. While there is evidence that peat burning indeed occurred as early as 1960, the drainage systems were less developed and the average burned layer depth most likely remained below 0.1 m (*Sorensen,* 1993). According to our estimates, the annual total carbon emissions from Indonesia range from 14 TgC/year (1962, 1974 and 1975) up to 1136 TgC/year in 1997. GFED version 2 estimates 1013, 278, 57 and 41 TgC for the years 1997, 1998, 1999 and 2000, respectively. These values are between 2 and 12 % lower than our results, which should be considered a very good agreement.

5.7. Australia

Table 8 compares recent estimates of burned areas and total carbon emissions from Australian fires. *Russel-Smith et al.* (2004) reported an annual mean of 37.3 Mha affected by fires across the tropical savannas in northern Australia from AVHRR imagery collated between 1997 and 2002. Annual burning extent ranged from 25 Mha in 1998 to 53 Mha in 2001, primarily due to inter-annual variability in monsoonal activity. *Spessa et al.* (2007) demonstrated the strong influence rainfall variability has on both the amount and moisture content of biomass available for burning across northern Australia, using AVHRR imagery applied to large scale rainfall gradients. Savanna fires occur during the dry season from about May to November every year. Late-dry season fires typically combust all dead grass and tree litter, and where sufficiently high in intensity to reach tree canopies, tree leaves and small branches as well. Most savanna grasses and tropical eucalypt trees are highly resistant to fires, and quickly grow back through seed banks (grasses) or resprouting (trees) (*Williams et al,* 2002). Other fire-prone regions are the arid grasslands in the central part of the continent (September through March), the subtropical landscapes along the east coast (September through January), and temperate forests in south-west

Table 8. Comparison of burned areas and carbon emissions from Australian fires

Year	Burned Area [Mha]	Carbon Emissions [TgC/year]	Fraction of Savanna fires	Comments	Reference
climatology	87	132	72%	estimate based on fire return interval	*Hurst et al.,* 1992
1999	41.8	$\leq$ 106	–	Northern Australian savanna only	*Russel-Smith et al.,* 1999
1997-2001	118	144	–	GFED	*van der Werf et al.,* 2003
2000	57	–	92%	GBA2000	*Tansey et al.,* 2004
2000	17.8	72	–	GWEM 1.2, GLOBSCAR	*Hoelzemann et al.,* 2004
2000	57	189	95%	GWEM 1.4, GBA2000	*Hoelzemann* (2006)
2000	33.9	109	–		*Ito and Penner,* 2004
1960-2000	8-55	43-312	95%		this study

and south-east Australia during extended drought periods (*Bradstock et al.* 2002). Across Australia, savanna burning contributes around 70% to the national extent of burning based on AVHRR imagery (B. Heath and R. Craig unpublished data, http://www.firewatch.dli.wa.gov.au; *Russell-Smith et al.,* 2004), yielding a continent-wide average of around 53 Mha burning per year. However, this figure is likely too conservative and subject to considerable uncertainty given that (i) coarse-resolution AVHRR sensors have problems detecting fires under denser tree canopies, characteristic of many Australian forests, and (ii) no published finer-resolution satellite mapping of fires in such forests exists for testing the AVHRR fire data.

According to *Hurst et al.* (1994) savanna fires contribute between 60 and 75% to the annual carbon release from fires, and more than half of this amount can be attributed to the monsoon tallgrass fires in Northern Australia.

Russel-Smith et al. (2003) analysed Northern Australian savanna fires for the year 1999 and derived a burned area of 41.8 Mha from AVHRR fire scar mapping. They estimate a fine fuel consumption of 212 Tg, which poses a limit of approximately 106 TgC on the total carbon emissions from this region. The burned areas derived from various global satellite data products differ by more than a factor of 6, but they center around 60-90 Mha (Table 8).

Reg-FIRM generates burned areas between 28 and 97 Mha/year for Australia. The variability of the Reg-FIRM results is consistent with estimates by *Cheney et al.* (1980) (cited by *Hurst et al.,* 1994), who report an increase in total burned area in Australia of a factor of 4 for extreme fire years. The average burned area of GFED version 1 (*van der Werf et al.,* 2003) exceeds all other estimates by about 20%, and it has only a small interannual variability in contrast to the Reg-FIRM results (total carbon emissions from GFED version 1 vary by less than 5% between 1997 and 2001). In version 2 of the GFED inventory (*van der Werf et al.,* 2006), the burned areas are in much better agreement with the other estimates and the interannual variability of burned area is about a factor of 3, values ranging from 25 Mha in 2003 to 78 Mha in 2001.

According to *Hurst et al.* (1994) most of the Australian vegetation has a fine fuel load below 3 t/ha. *Russel-Smith et al.* (2003) derived their estimate of fuel consumption on fine fuels (grass and litter) only and note that some fraction of coarse fuel may also burn occasionally. *Hoelzemann et al.* (2004) and *Ito and Penner* (2004) give average carbon release for wooded savanna (grasslands) of 3.8 (1.0) and 3.0 (1.5) tC/ha, respectively.

For the RETRO inventory we adopt a uniform carbon consumption of 2.5 tC/ha for grasslands and wooded savanna. The MODIS landcover data set classifies the Northern Australian savanna as grasslands, whereas the other regions with burning are mostly labelled as "wooded". In order to qualitatively reproduce the burning patterns observed in satellite data sets and in Reg-FIRM, we assume that 69% of the total burned area computed by Reg-FIRM are grasslands, 30% are wooded savanna, and 1% is forest. Forests are assigned a net carbon emission flux of 15 tC/ha.

The geographical distribution of fires is performed randomly within the three ecosystem classes using the Reg-FIRM fire danger index as a weighting function and the seasonality of the GWEM 1.4 inventory. Total carbon emissions thus calculated range from 83 TgC/year (1968) to 295 TgC/year (1980), the average amounts to 169 TgC/year. The geographical variability of emissions over the course of a year is in good agreement with the satellite-derived data sets of GWEM 1.4 and GFED except that fires in eastern Australia may be overestimated during austral winter. The RETRO inventory also sees fewer fires in the Gibson and Great Victoria deserts. Here, the satellite-derived data sets should perhaps be scrutinized again for possible false detection of fires on hot surfaces.

Table 9 compares the annual carbon emission estimates from our study with the values of GFED version 2 (*van der Werf et al.,* 2006). While there is excellent agreement for the year 1997, the deviation is larger for 1999 and 2000 and almost a factor of 2 for the year 1998. The reasons for these discrepancies are presently unclear.

6. Conclusions

The fire situation, fire regimes and their historical developments are very different in different world regions. Up to now very little quantitative information is available to reliably assess average emission fluxes and their interannual variability on a regional basis. While we found at times excellent agreement with some recent literature values (most notably with the GFED version 2 inventory by *van der Werf et al.,* 2006), this agreement is often fortuitous and does not always reflect the true uncertainty of the bottom-up emissions estimate (see also *Hoelzemann,* 2006). Nevertheless, the second version of the RETRO inventory as is described in this paper probably reflects the state-of-the-art in terms of estimating fire emissions over a multi-decadal period and consistently across the globe. Many documented extreme fire events are captured in this inventory, although the magnitude of their emission enhancements may be underestimated from time to time. Specifically, the RETRO long-term simulations with three different global chemistry transport models indicate that monthly mean anomalies of surface CO measured by the NOAA-ESRL network are generally well captured, but the magnitude of the extreme enhancement in 1998, which has been attributed to boreal forest fires, is underestimated by about 50 %. The inventory could be further improved by expanding the underlying database to include more detailed information on ecosystems and their carbon stocks and burning behavior. This will have to remain a subject for future studies.

Table 9. Comparison of total carbon emissions from Australian fires for the late 1990s

Carbon emissions [TgC/year]				Comments	Reference
1997	1998	1999	2000		
175	99	137	158	GFED version 2	*van der Werf et al.*, 2006
171	178	177	194		this study

References

Achard, F., H.D. Eva, H.-J. Stibig, P. Mayaux, J. Gallego, T. Richards, and J.-P. Malingreau (2002), Determination of Deforestation Rates of the World's Humid Tropical Forests, *Science, 297*, 999-1002.

Achard, F., H.D. Eva, P. Mayeaux, H.-J. Stibig, and A. Belward (2004), Improved estimates of net carbon emissions from land cover change in the tropics for the 1990s, *Global Biogeochem. Cycles, 18*, (GB2008), doi:10.1029/2003GB002142.

Amiro, B.D., J.B. Todd, B.M. Wotton, K.A. Logan, M.D. Flannigan, B.J. Stocks, J.A. Mason, D.L. Martell, and K.G. Hirsch (2001), Direct carbon emissions from Canadian forest fires, 1959 to 1999, *Can. J. For. Res., 31*, 512-525.

Andreae, M.O. (1991), Biomass burning: Its history, use, and distribution, and its impact on environmental quality and climate, In: J.S. Levine (ed.), Global biomass burning, Atmospheric, climatic, and biospheric implications, pp. 3-21, MIT Press, Cambridge, MA.

Andreae, M.O., and P. Merlet (2001), Emission of trace gases and aerosols from biomass burning, *Global Biogeochem. Cycles, 15*, 4, 955-966.

Anyamba, A., C.O. Justice, C.J. Tucker, and R. Mahoney (2003), Seasonal to interannual variability of vegetation and fires at SAFARI 2000 sites inferred from advanced very high resolution radiometer time series data, *J. Geophys. Res., 108*(D13), 8507, doi:10.1029/2002JD002464.

Arino, O., and J.-M. Rosaz (1999), 1997 and 1998 World ATSR Fire Atlas using ERS-2 ATSR-2 data, Proceedings of the Joint Fire Science Conference, Boise, 15-17 June, 1999.

Bahugana, V.K. and S. Singh (2002), Fire situation in India, *Int. Forest Fire News*, 26, 23-27.

Barbosa, P.M., D. Stroppiana, J.M. Gregoire, J.M.C. Pereira (1999), An assessment of vegetation fire in Africa (1981-1991): Burned areas, burned biomass, and atmospheric emissions, *Global Biogeochem. Cycles*, 13(4), 933-950.

Boschetti, L., H.D. Eva, P.A. Brivio, and J.M. Gregoire (2004), Lessons to be learned from the comparison of three satellite-derived biomass burning products, *Geophys. Res. Lett., 31*, L21501, doi:10.1029/2004GL021229.

Bradstock, R., J. Williams, and A.M. Gill (2002), Flammable Australia: Fire regimes and biodiversity of a continent, 486 pp., Cambridge University Press, Cambridge, UK.

Cardoso, M.F., G.C. Hurtt, B. Moore III, C.A. Nobre, and E.M. Prins (2003), Projecting future fire activity in Amazonia, *Global Change Biology, 9*, 656-669.

Catchpole, W. (2002), Fire properties and burn patterns in heterogenous landscapes, In: Flammable Australia: Fire regimes and biodiversity of a continent, R. Bradstock, J. Williams, and A. M. Gill (eds.), pp. 49-76, Cambridge University Press, Cambridge, UK.

Cheney, N.P., R.J. Raison, and P.K. Khanna (1980), Release of carbon to the atmosphere in Australian vegetation fires, in: Carbon dioxide and climate: Australian Reearch, G.I. Pearman (ed.), pp. 153-158, Australian Academy of Science, Canberra.

Cheney, P., J. Gould, and W. Catchpole (1993), The influence of fuel, weather and fire shape variables on fire spread in grasslands, *International J. Wildland Fire, 3*, 31-44.

Cochrane, M.A. (2002), Spreading like Wildfire - tropical forest fires in Latin America and the Caribbean: Prevention, assessment and early warning, UNEP report, 96 pp., ISBN 92-807-1818-7.

Cochrane, M.A. (2003), Fire science for rainforests, *Nature, 421*, 913-919.

Conard, S.G., A.I. Sukhinin, B.J. Stocks, D.R. Cahoon, E.P. Davidenko, and G.A. Ivanova (2002), Determining effects of area burned and fire severity on carbon cycling and emissions in Siberia, *Climatic Change, 55*(1-2), 197-211.

Duncan, B.N., R.V. Martin, A.C. Staudt, R. Yevich, J.A. Logan (2003), Interannual and seasonal variability of biomass burning emissions constrained by satellite observations, *J. Geophys. Res.*, 108(D2), doi:10.1029/2002JD002378.

Dwyer, E., S. Pinnock, J-M. Grgoire, J.M.C. Pereira (2000), Global spatial and temporal distribution of vegetation fire as determined from satellite observations. *Int. J. Remote Sensing, 21*, 1289-1302.

Etheridge, D.M., L.P. Steele, R.L. Langenfelds, R.J. Francey, J.M. Barnola, V.I. Morgan (1996), Natural and anthropogenic changes in atmospheric CO2 over the last 1000 years from air in Antarctic ice and firn, *J. Geophys. Res., 101 (D2)*, 4115-4128.

FAO (1991), The Digitized Soil Map of the World (Release 1.0), Food and Agriculture Organization of the United Nations, 67/1.

FAO (2003), WRB Map of World Soil Resources, Land and Water Development Division AGL, Rome, Italy, Food and Agriculture Organisation of the United Nations. Available at http://www.fao.org/ag/agl/agll/wrb/soilres.htm.

French, N.H.F., E.S. Kasischke, and D.G. Williams (2003), Variability in the emission of carbon-based trace gases from wildfire in the Alaskan boreal forest, *J. Geophys. Res., 108*(D1), 8151, doi:10.1029/2001JD000480.

Friedl, M.A., D.K. McIver, J.C.F. Hodges, X.Y. Zhang, D. Muchoney, A.H. Strahler, C.E. Woodcock, S. Gopal, A. Schneider, A. Cooper, A. Baccini, F. Gao, and C. Schaaf (2002), Global landcover mapping from MODIS: algorithms and early results, *Int. J. Remote Sens., 83*, 287-302.

Gerten, D., S. Schaphoff, U. Haberlandt, W. Lucht, and S. Sitch (2004), Terrestrial vegetation an large-scale water balance: Hydrological evaluation of a dynamic global vegetation model, *Journal of Hydrology, 286*, 249-270.

Goldammer, J.G., and V.V. Fuyaev (1996), Fire in Ecosystems of Boreal Eurasia, 528 pp., Kluwer Academic Publishers, Dordrecht, The Netherlands.

Goldammer, J. (2003), Russian Federation Fire 2002 Special, Part I: The wildland fire season 2002 in the Russian Federation, An assessment by the Global Fire Monitoring Center (GFMC), *Int. Forest Fire News, 28*, 2-14.

Goldammer, J., A. Sukhinin and I. Csiszar (2004), The Current Fire Situation in the Russian Federation: Implications for Enhancing International and Regional Cooperation in the UN Framework and the Global Programs on Fire Monitoring and Assessment. International Forest Fire News No. 29, 89-111.

Goldammer, J. (2006), Global Forest Resources Assessment 2005: Report on fires in the Central Asian region and adjacent countries, Working Paper FM/16/E, Food and Agricultural Organisation, Rome, Italy. Available at http://www.gfmc.org.

Goldewijk, K.K. (2005), Three centuries of global population growth: A spatial referenced population density database for 1700-2000, *Population and Environment, 26*, 4, 343-367.

Hao, W.M., and M.H. Liu (1994), Spatial and temporal distribution of tropical biomass burning, *Global Biogeochem. Cycles, 8*, 495-503.

Heald, C.L., D.J. Jacob, P.I. Palmer, M.J. Evans, G.W. Sachse, H.B. Singh, and D.R. Blake (2003), Biomass burning emission inventory with daily resolution: Application to aircraft observations of Asian outflow, *J. Geophys. Res., 108*(D21), 8811, doi:10.1029/2002JD003082.

Heald, C.L., D.J. Jacob, D.B.A. Jones, P.I. Palmer, J.A. Logan, D.G. Streets, G.W. Sachse, J.C. Gille, R.N. Hoffman, and T. Nehrkorn (2004), Comparative inverse analysis of satellite (MOPITT) and aircraft (TRACE-P) observations to estimate Asian sources of carbon monoxide, *J. Geophys. Res., 109*(D23306), doi:10.1029/2004JD005185.

Heil, A., B. Langmann, and E. Aldrian (2005), Indonesian peat and vegetation fire emissions: Study on factors influencing large-scale smoke haze pollution using a regional atmospheric chemistry model. *Mitig. Adapt. Strat. Glob. Change, 12*, (1), 113-133.

Hoelzemann, J.J., M.G. Schultz, G.P. Brasseur, and C. Granier (2004), Global wildland fire emission model (GWEM): Evaluating the use of global area burnt satellite data, *J. Geophys. Res., 109*(D14S04), doi:10.1029/2003JD003666.

Hoelzemann, J.J. (2006), Global wildland fire emission modeling for atmospheric chemistry studies, *PhD thesis*, Hamburg. Available as Report on Earth System Sciences, 28/2006 at http://www.mpimet.mpg.de.

Holmes, D.A. (2002), Indonesia: Where have all the forests gone?, Environment and Social Development, East Asia and Pacific Region, Discussion paper, The World Bank, Washington. (available at http://www.worldbank.org/)

Houghton, R.A. (2003), Revised estimates of the annual net flux of carbon to the atmosphere from changes in land use and land management 1850–2000, *Tellus, 55B*, 378-390.

Houghton, R.A. (2005), Aboveground forest biomass and the global carbon balance, *Global Change Biology, 11*, 945-958, doi:10.1111/j.1365-2486.2005.00955.x.

Hurst, D.F., D.W.T. Griffith, and G.D. Cook (1994), Trace gas emissions from biomass burning in tropical Australian savannas, *J. Geophys. Res., 99*(D8), 16,441-16,456.

Ito, A., J.E. Penner (2004), Global estimates of biomass burning emissions based on satellite imagery for the year 2000, *J. Geophys. Res.*, 109(D14), doi:10.1029/2003JD004423.

Ito, A., A. Ito, H. Akimoto (2007), Seasonal and interannual variations in CO and BC emissions from open biomass burning in Southern Africa during 1998-2005, *Global Biogeochem. Cycles, 21*, GB2011, doi:10.1029/2006GB002848.

Kasischke, E.S., E.J. Hyer, P.C. Novelli, L.P. Bruhwiler, N.H.F. French, A.I. Sukhinin, J.H. Hewson, and B.J. Stocks (2005), Influences of boreal fire emissions on Northern hemisphere atmospheric carbon and carbon monoxide, *Global Biogeochem. Cycles, 19*, GB1012, doi:10.1029/2004GB002300.

Keeling, C.D., J.F.S. Chin, T.P. Whorf (1996), Increased activity of northern vegetation inferred from atmospheric CO_2 measurements, *Nature, 382 (6587)*, 146-149.

Keeling, C.D. and T.P. Whorf (2005), Atmospheric CO_2 records from sites in the SIO air sampling network, in Trends: A Compendium of Data on Global Change, *C*arbon Dioxide Information Analysis Center, Oak Ridge National Laboratory, U.S. Department of Energy, Oak Ridge, Tenn., U.S.A.

Loveland, T.R., B.C. Reed, J.F. Brown, D.O. Ohlen, J. Zhu, L. Yang, and J.W. Merchant (2000), Development of a global landcover characteristics database and IGBP DISCover from 1 km AVHRR data, *Int. J. Remote Sens., 21*(6-7), 1303-1330.

McGuire, A., S. Sitch, J.S. Clein, R. Dargaville, G. Esser, J. Foley, M. Heimann, F. Joos, J. Kaplan, D.W. Kicklighter, R.A. Meier, J.M. Melillo, B. Moore, I.C. Prentice, N. Ramankutty, T. Reichenau, A. Schloss, H. Tian, L.J. Williams, U. Wittenberg (2001), Carbon balance of the terrestrial biosphere in the twentiethy century: analysis of CO_2, climate and land use effects with four process-based ecosystem models, *Global Biogeochem. Cycles, 15*, 1, 183-206.

Merida, J.-C. (1999), Descripción de los modelos combustibles usados en la prediccion del comportamiento 27 del fuego, Àrea de Defensa Contra Incendios Forestales, Ministerio de Medio Ambiente España.

Mitchell, T.D., T.R. Carter, P.D. Jones, M. Hulme, and M. New (2003), A comprehensive set of high-resolution grids of monthly climate for Europe and the globe: the observed record (1901-2000) and 16 scenarios (2001-2100), available at: http://www.cru.uea.ac.uk/timm/data/index.html.

MoF (Ministry of Forestry Indonesia) (2003), Statistik Kehutanan Indonesia 2003, Departemen Kehutanan, Sekretariat Jenderal dan Biro Perencanaan, Jakarta, Indonesia.

Mueller-Dombois, D., and J.G. Goldammer (1990), Fire in tropical ecosystems and global environmental change: An introduction, In: J.G. Goldammer (ed.), Fire in the tropical biota, Springer-Verlag, Berlin, Heidelberg.

Page, S.E., F. Siegert, J.O. Rieley, H.D.V. Boehm, A. Jaya, S. Limin (2002), The amount of carbon released from peat and forest fires in Indonesia during 1997, *Nature*, 420(6911), 61-65.

Palacios-Orueta, A., A. Parra, E. Chuvieco, and C. Carmona-Moreno (2004), Remote sensing and geographic information systems methods for global spatiotemporal modeling of biomass burning emissions: Assessment in the African continent, *J. Geophys. Res., 109*(D14S09), doi:10.1029/2004JD004734.

Pétron, G., C. Granier, B. Khattatov, V. Yudin, J.-F. Lamarque, L. Emmons, J. Gille, and D.P. Edwards, (2004), Monthly CO surface sources inventory based on the 2000-2001 MOPITT satellite data, *Geophys. Res. Lett., 31*(L21107), doi:10.1029/2004GL020560.

Potter, C., V. Brooks-Genovese, S. Klooster, and A. Torregrosa (2002), Biomass burning emissions of reactive gases estimated from satellite data analysis and ecosystem modeling for the Brazilian Amazon region, *J. Geophys. Res., 107*(D20), 8056, doi:10.1029/2000JD000250.

Prins, E.M., W.P. Menzel, and D.E. Ward (1996), GOES-8 ABBA diurnal fire monitoring during SCAR-B, *Smoke/Sulfate, Clouds and Radiation – Brazil (SCAR-B) Proceedings*, Fortaleza, Transtec Editorial, 153-157, 4-8 November 1996.

Prins, E.M., J.M. Feltz, W.P. Menzel, and D.E. Ward (1998), An overview of GOES-8 diurnal fire and smoke results for SCAR-B and 1995 fire season in South America, *J. Geophys. Res., 103*, D24, 31821-31835.

Pyne, S., P. Andrews, and R. Laven (1996), Introduction to Wildland Fire, 808 pp., Wiley and Sons, New York.

Qadri, S.T. (ed.) (2001), Fire, Smoke, and Haze: The ASEAN Response Strategy. Asian Development Bank and Association of Southeast Asian Nations (ASEAN), Manila, Philippines. Available at http://www.adb.org/Documents/Reports/Fire_Smoke_Haze/.

Reid, J.S., R. Koppmann, T.F. Eck, and D.P. Eleuterio (2005), A review of biomass burning emissions part II: Intensive physical properties of biomass burning emissions, *Atmos. Chem. Phys., 5*, 799-825.

Roberts, G., M.J. Wooster, G.L.W. Perry, N. Drake, L.-M. Rebelo, F. Dipotso (2005), Retrieval of biomass combustion rates and totals from fire radiative power observations: application to southern Africa using geostationary SEVIRI Imagery, *J. Geophys. Res., 110*, D21111: doi: 10.1029/2005JD006018.

Robinson, J.M. (1989), On uncertainty in the computation of global emissions from biomass burning, *Climatic Change, 14*, 243-261.

Rogers, C.M., and K.P. Bowman (2001), Transport of smoke from the Central American fires of 1998, *J. Geophys. Res., 106*(D22), 28,357-28,368.

Russel-Smith, J., A.C. Edwards, and G.D. Cook (2003), Reliability of biomass burning estimates from savanna fires: Biomass burning in Northern Australia during the 1999 Biomass Burning and Lightning Experiment B field campaign, *J. Geophys. Res., 108*(D3), 8405, doi:10.1029/2001JD000787.

Russell-Smith, J., C. Yates, A. Edwards, G.E. Allan, G.D. Cook, P. Cooke, R. Craig, B. Heath, and R. Smith (2004), Contemporary fire regimes of northern Australia, 1997-2001: Change since Aboriginal occupancy, challenges for sustainable management, *International J. Wildland Fire, 12*, 283-297.

Scholes, R.J., J. Kendall, and C.O. Justice (1996), The quantity of biomass burned in southern Africa, *J. Geophys. Res., 101*, D19, 23667-23676.

Shimada, S., H. Takahashi, A. Haraguchi, and M. Kaneko (2001), The carbon content characteristics of tropical peats in Central Kalimantan, Indonesia: Estimating their spatial variability in density, *Biogeochemistry, 53*, 3, 249-267.

Simon, M., S. Plummer, F. Fierens, J.J. Hoelzemann, and O. Arino (2004), Burnt area detection at global scale using ATSR-2: The GLOBSCAR products and their qualification, *J. Geophys. Res., 109*, D14S02, doi:10.1029/2003JD003622.

Sitch, S., B. Smith, I.C. Prentice, A. Arneth, A. Bondeau, W. Cramer, J.O. Kaplan, S. Levis, W. Lucht, M.T. Sykes, K. Thonicke, and S. Venevsky (2003), Evaluation of ecosystem dynamics, plant geography and terrestrial carbon cycling in the LPJ Dynamic Global Vegetation Model, *Global Change Biology, 9*, 161-185.

Soja, A.J., W.R. Cofer, H.H. Shugart, A.I. Sukhinin, P.W. Stackhouse, D.J. McRae, S.G. Conard (2004), Estimating fire emissions and disparities in boreal Siberia (1998-2002), *J. Geophys. Res., 109*(D14), doi:10.1029/2004JD004570.

Sorensen, K.W. (1993), Indonesian peat swamp forests and their role as a carbon sink, *Chemosphere, 27*, 1065-1082.

Spessa, A., B. McBeth, K. Thonicke, and I.C. Prentice (2003), Modelling the relationship between fire frequency, rainfall and vegetation in the Kimberleys region Australia, using a fire model coupled to a DGVM, In: J.G. Goldammer, and D.X. Viegas (eds), Proceedings of the 3rd International Wildland Fire Conference, 4-6 Oct. 2003, Sydney, Australia.

Spessa, A., B. McBeth, and I.C. Prentice (2005), Relationships among fire frequency, rainfall and vegetation patterns in the wet-dry tropics of northern Australia: An analysis based on NOAA-AVHRR data, *Global Ecology and Biogeography, 14*, 439-454.

Stocks, B.J. (1991), The extent and impact of forest fires in northern circumpolar countries. In: Global biomass burning: Atmospheric, climatic, and biospheric implications, J.S. Levine (ed.), The MIT press, Cambridge, MA, pp. 197-202.

Stocks, B.J., M.A. Fosberg, T.J. Lynham, L. Mearns, B.M. Wotton, Q. Yang, J.-Z. Zin, K. Lawrence, G.R. Hartley, J.A. Mason, and D.W. McKenney (1998), Climate change and forest fire potential in russian and canadian boreal forests, *Climatic Change, 38*, 1-13.

Stocks, B.J., J.A. Mason, J.B. Todd, E.M. Bosch, B.M. Wotton, B.D. Amiro, M.D. Flannigan, K.G. Hirsch, K.A. Logan, D.L. Martell, and W.R. Skinner (2003), Large forest fires in Canada, 1959-1997, *J. Geophys. Res., 108*(D1), 8149, doi:10.1029/2001JD000484.

Stocks, B.J. (2004), Forest fires in the boreal zone: Climate change and carbon implications, *Int. Forest Fire News, 31*, 121-131.

Sukhinin, A.I., N.H.F. French, E.S. Kaschischke, J.H. Hewson, A.J. Soja, I.A. Csiszar, E.J. Hyer, T. Loboda, S.G. Conrad, V.I. Romasko, E.A. Paclichenko, S.I. Miskiv, and O.A. Slinkina (2004), AVHRR-based mapping of fires in Russia: New products for fire management and carbon cycle studies, *Remote Sensing of Environment, 93*, 546-564.

Tacconi, L. (2003), Fires in Indonesia: Causes, costs, and policy implications, *CIFOR Occasional Papers, 38*, Center for International Forestry Research, Bogor, Indonesia.

Tansey, K., J.-M. Grégoire, D. Stroppiana, A. Sousa, J. Silva, J.M.C. Pereira, L. Boschetti, M. Maggi, P.A. Brivio, R. Fraser, S. Flasse, D. Ershov, E. Binaghi, D. Graetz, and P. Peduzzi (2004), Vegetation burning in the year 2000: Global burned area estimates from SPOT VEGETATION data, *J. Geophys. Res., 109*, D14S03, doi:10.1029/2003JD003598.

Telitsyn, H.P. (1996), A mathematical model of spread in high-intensity forest fires, In: J.G. Goldammer, and V.V. Fuyaev (eds.), Fire in Ecosystems of Boreal Eurasia, pp. 139-150, Kluwer Academic Publishers, Dordrecht, The Netherlands.

Thonicke, K., S. Venevsky, S. Sitch, and W. Cramer (2001), The role of fire disturbance for global vegetation dynamics: coupling fire into a dynamic global vegetation model, *Global Ecology and Biogeography, 10*, 661-677.

Thonicke, K., and W. Cramer (2006), honicke, K., Cramer, W. (2006). Long-term Trends in Vegetation Dynamics and Forest Fires in Brandenburg (Germany) Under a Changing Climate *Natural Hazards, 38*, 283-300.

Toma, T., P. Matius, Hastaniah, Y. Kiyono, R. Watanabe, Y. Okimori (2000), Dynamics of burned lowland dipterocarp forest stands in Bukit Soeharto, East Kalimantan, Ecological Studies, vol. 140, Guhardja et al. (eds), Rainforest Ecosystems of East Kalimantan: El Niño, drought, fire, and human impacts, Springer-Verlag, Tokyo.

van der Werf, G., J.T. Randerson, G.J. Collatz, and L. Giglio (2003), Carbon emissions from fires in tropical and subtropical ecosystems, *Global Change Biology, 9*, 547-562.

van der Werf, G., J.T. Randerson, G.J. Collatz, L. Giglio, P.S. Kasibhatla, A.F. Arellano, S.C. Olsen, and E.S. Kasischke (2004), Continental-scale partitioning of fire emissions during the 1997 to 2001 El Niño/La Niña period, *Science, 303*, 73-76, 2004.

van der Werf, G., J.T. Randerson, L. Giglio, G.J. Collatz, P.S. Kasibhatla, and A.F. Arellano, Jr. (2006), Interannual variability in global biomass burning emissions from 1997 to 2004, *Atmos. Chem. Phys., 6*, 3423-3441.

Venevsky, S., K. Thonicke, S. Sitch, and W. Cramer (2002), Simulating fire regimes in human-dominated ecosystems: Iberian Peninsula case study, *Global Change Biology, 8*, 984-998.

Vogel C. (2004), Modelling the relationships among fire, rainfall and vegetation in the Western USA, using a regional fire model coupled to a DGVM, Unpublished Diplomarbeit (MSc) thesis, Friedrich-Schiller-University, Jena.

Williams, R., A. Griffiths, and G. Allan (2002), Fire regimes and biodiversity in the savannas of northern Australia, In: Flammable Australia: Fire regimes and biodiversity of a continent, R. Bradstock, J. Williams, and A. M. Gill (eds.), pp. 281-304, Cambridge University Press, Cambridge, UK.

Wolter, K., and M.S. Timlin (1998), Measuring the strength of ENSO: How does 1997/98 rank?, *Weather, 53*, 315-324. (data available at http://www.cdc.noaa.gov/people/klaus.wolter/MEI/table.html)

Wooster, M. J., and Y. H. Zhang (2004), Boreal forest fires burn less intensely in Russia than in North America, Geophys. Res. Lett., 31, L20505, doi:10.1029/2004GL020805.

Wooster, M.J., G. Roberts, G. Perry, and Y.J. Kaufman (2005), Retrieval of biomass combustion rates and totals from fire radiative power observations: calibration relationships between biomass consumption and fire radiative energy release, *J. Geophys. Res., 110*, D21111: doi: 10.1029/2005JD006318.

Zobler, L. (1986), A world soil file for global climate modelling, NASA Technical Memorandum, 87802, 32.

Zwenzner H. (2004), Simulation of fire-vegetation-rainfall interactions in the Australian wet-dry tropics, using a regional fire model linked to a DGVM, Unpublished Diplomarbeit (MSc) thesis, Friedrich-Schiller-University, Jena.